

# Optimizing DF Cognitive Radio Networks with Full-Duplex-Enabled Energy Access Points

Hong Xing, Xin Kang, Kai-Kit Wong, and Arumugam Nallanathan

## Abstract

With the recent advances in radio frequency (RF) energy harvesting (EH) technologies, wireless powered cooperative cognitive radio network (CCRN) has drawn an upsurge of interest for improving the spectrum utilization with incentive to motivate joint information and energy cooperation between the primary and secondary systems. Dedicated energy beamforming (EB) is aimed for remedying the low efficiency of wireless power transfer (WPT), which nevertheless arouses out-of-band EH phases and thus low cooperation efficiency. To address this issue, in this paper, we consider a novel RF EH CCRN aided by full-duplex (FD)-enabled energy access points (EAPs) that can cooperate to wireless charge the secondary transmitter (ST) while concurrently receiving primary transmitter (PT)'s signal in the first transmission phase, and to perform decode-and-forward (DF) relaying in the second transmission phase. We investigate a weighted sum-rate maximization problem subject to the transmitting power constraints as well as a total cost constraint using successive convex approximation (SCA) techniques. A zero-forcing (ZF) based suboptimal scheme that requires only local CSIs for the EAPs to obtain their optimum receive beamforming is also derived. Various tradeoffs between the weighted sum-rate and other system parameters are provided in numerical results to corroborate the effectiveness of the proposed solutions against the benchmark ones.

## Index Terms

cognitive radio, cooperative communication, full-duplex, decode-and-forward, D.C. programming, successive convex approximation, power splitting, energy harvesting.

## I. INTRODUCTION

With the rapid development of wireless services and applications, the demand for frequency resources has dramatically increased. How to accommodate these new wireless services and

Part of this paper has been accepted by the IEEE Global Communications Conference (GLOBECOM), 2016.

H. Xing and A. Nallanathan are with the Department of Informatics, King's College London, London, WC2R 2LS, UK (e-mails: hong.xing@kcl.ac.uk; arumugam.nallanathan@kcl.ac.uk).

X. Kang is with the National Key Laboratory of Science and Technology on Communications, University of Electronic Science and Technology of China, Chengdu, 611731, China (e-mail: kangxin83@gmail.com).

K.-K. Wong is with the Department of Electronic and Electrical Engineering, University College London, London, WC1E 6BT, UK (e-mail: kai-kit.wong@ucl.ac.uk).

applications within the limited radio spectrum becomes a big challenge facing the modern society [1]. The compelling need to establish more flexible spectrum regulations motivates the advent of cognitive radio (CR) [2]. Cooperative cognitive radio networks (CCRN) further pave way to improve the spectrum efficiency of a CR system by advocating cooperation between the primary and secondary systems for mutual benefits. Compared with classical CR approaches [3], CCRN enables cooperative gains on top of CR in the sense that the secondary transmitter (ST) helps to provide the diversity and enhance the performance of primary transmission via relaying the primary user (PU)'s message while being allowed to access the PU's spectrum.

Although the conventional CCRN benefits from information-level cooperation, its implementation in real world might be limited due to STs' power constraints, especially when the STs are low-power devices, such as energy constrained wireless sensors and small cell relays. With the advent of various energy harvesting (EH) technologies, CCRN has now been envisioned to improve the overall system spectrum efficiency by enabling both information-level and energy-level cooperation [4]. Apart from the natural energy sources such as solar and wind that is intermittent due to the environmental change, ambient radio signal has recently been exploited as a new viable source for wireless energy harvesting (WEH) (see [5] and references therein). RF-enabled WET has many preferred advantages. For example, compared with other induction-based WET technologies, WEH can power wireless devices to relatively longer distance exploiting the far-field propagation properties of electromagnetic (EM) wave (e.g., commercial chips available for tens of microwatts ( $\mu\text{W}$ ) RF power transferred over 12m [6]), while the associated transceiver designs are more flexible with the transmitting power, waveforms, occupied resource blocks fully controlled to accommodate different physical conditions. Joint information and energy cooperation in CR networks has thus been actively investigated in many WEH-enabled scenarios, e.g., [7–10].

The benefit of radio frequency (RF)-powered CCRN is nevertheless compromised by the low wireless power transfer (WPT) efficiency mainly due to the severe RF signal attenuation over distance. One way to improve the WPT efficiency is to employ multiple antennas at the ST, which can improve the EH efficiency of the secondary system [8]. The other way to boost the WPT efficiency is to power the ST via WPT from the dedicated energy/hybrid access point (EAP/HAP) [9] in addition to the PU. However, the above works all assume that the involved devices operate in half-duplex (HD) mode, which provides more reliable power supplies for CCRN at the expense of some spectrum efficiency. In continuous effort to address this issue, full-duplex (FD)-enabled communications with wireless information and power transfer has sparked an upsurge of interest thanks to the advance in antenna technologies (see [11–15] and references therein).

In this paper, we consider a spectrum-sharing decode-and-forward (DF) relaying CR network consisting of one pair of primary transmitter (PT) and primary receiver (PR), and one pair of

multiple-input multiple-output (MIMO) secondary users (SUs). A number of multi-antenna FD EAPs are coordinated to transfer wireless power to the ST while simultaneously listening to information sent from the PT in the first transmission phase, and decode then forward the PT's message to the PR in HD mode in the second transmission phase. The ST is required to assist the primary transmission and earn the rights to access the PU's spectrum in return; the EAPs are paid by the system as an incentive to support the cooperative WPT and wireless information transfer (WIT). We assume that there is no direct link between the PT and the PR due to severe pathloss [14], and the perfect<sup>1</sup> global channel state information (CSI) known at a centralized coordination point who is in charge of acquiring global CSI from the dedicated nodes<sup>2</sup> via backhauls and implementing the algorithm accordingly in every transmission block (assumed to be equal to the channel coherence time).

Compared with [7] investigating joint opportunistic EH and spectrum access, we focus on *overlay* CR transmission, which allows for primary messages known at the ST *a priori* due to the first-slot transmission, so that the ST can precancel the interference caused to the secondary receiver (SR) by some non-linear precoding techniques, e.g., dirty-paper coding (DPC). In this case, beamforming precoding for the primary and the secondary messages at the ST needs to be jointly designed to achieve cooperative gain. Furthermore, although overlay cognitive WPCN has been considered in [9] with dedicated WPT, the HAP was only equipped with one antenna therein, and therefore their transmission policy is not applicable to ours with multi-antennas. In [8], the multi-antenna ST received information from the primary transmitter (PT) and was also fed with energy by the PT using PS and/or time switching (TS) receiver. However, the energy received by the ST was not intended for WPT and thus the RF EH capability and the cooperative gains was limited. By contrast, the deployment of cooperative FD-enabled EAPs intended for WPT in this paper breaks this bottleneck. A wireless powered communication network (WPCN) with an FD-enabled HAP and a set of WEH-enabled time division multiple access (TDMA) users was investigated in [15]. However perfect self interference (SI) cancellation between the transmitting and receiving antennas of the HAP was assumed therein, which is nevertheless not achievable in practice even with the state-of-the-art FD technique [18].

A similar setup was considered in [19], whereas our work differs from it mainly in two folds. First, the considered EAPs in this paper are FD empowered so that they fundamentally improve the spectral efficiency of the CCRN system of interest. Second, compared with the non-

<sup>1</sup>We assume perfect CSI at the Tx in this paper as in [8, 9, 11, 12], and thus the proposed transmission protocol design yields theoretical upper-bound. More practical design for wireless powered MIMO communication taking channel uncertainties into account can be referred to [16] and references therein.

<sup>2</sup>The dedicated nodes are assumed to be those non energy-limited thereby performing channel estimation in line with [17] and then reporting the corresponding CSI to the centralized coordinator connected by backhauls.

cooperative EAPs whose power levels are binary (on or off) in [19], we exploit EAP-assisted cooperation in both WPT and WIT phases via continuous power control, which is an extension to the non-cooperative model. The main contributions of this paper are summarized as follows.

- The weighted sum-rate of the FD EAPs-aided CCRN system is maximized using successive convex approximation (SCA) techniques subject to per-EAP power constraints for WPT and WIT, respectively, the ST's transmitting power constraint, and a practical cost budget that constrains the payment made to the EAPs for their dedicated WPT and WIT.
- The centralized optimization enables cooperation among the EAPs to effectively mitigate the interference with ST's information decoding (ID), and the SI that degrades EAPs' reception of the PT's signal.
- A low-complexity suboptimal design locally nulling out the SI at the EAPs is also developed in order to reduce the computational complexity of the iterative algorithm, and is validated by computer simulations to yield performance with little gap to that achieved by the proposed iterative solutions.
- Various tradeoffs, e.g., priority between primary and secondary transmissions, energy and cost allocations between WPT and WIT, are studied by solving the optimization problems, and evaluated by simulations to provide useful insights for system design in practice.

The remainder of the paper is organized as follows: Section II and III introduces the system model of the CCRN assisted by FD-enabled EAPs, and formulates the weighted sum-rate maximization problem, respectively. Section IV investigates the feasibility of a tractable reformulation of the original problem; proposes an SCA-based iterative solution along with a suboptimal scheme based upon zero-forcing (ZF) the SI. Benchmark schemes are studied in Section V. Section VI provides numerical results comparing the performance achieved by different schemes. Finally, Section VII concludes the paper.

*Notation*—We use the upper case boldface letters for matrices and lower case boldface letters for vectors.  $(\cdot)^T$ ,  $(\cdot)^H$ , and  $\text{Tr}(\cdot)$  denote the transpose, conjugate transpose, and trace operations on matrices, respectively.  $\|\cdot\|_p$  is  $\ell^p$ -norm of a vector with  $p = 2$  by default. The Kronecker product of two matrices is denoted by  $\otimes$ .  $\mathbf{A} \succeq 0$  indicates that  $\mathbf{A}$  is a positive semidefinite (PSD) matrix, and  $\mathbf{I}$  denotes an identity matrix with appropriate size.  $\mathbb{E}[\cdot]$  stands for the statistical expectation of a random variable (RV). In addition,  $\mathbb{C}(\mathbb{R})^{x \times y}$  stands for the field of complex (real) matrices with dimension  $x \times y$ , and  $\mathbb{Z}$  is the set of integer.  $(\cdot)^*$  means the optimum solution.

## II. SYSTEM MODEL

In this paper, we consider a WEH-enabled CCRN that consists of one primary transmitter-receiver pair, one secondary transmitter-receiver pair, and a set of FD-enabled EAPs denoted by  $\mathcal{K} = \{1, \dots, K\}$  as shown in Fig. 1. The PT and the PR are equipped with one antenna each,

while the ST and the SR are equipped with  $N$  and  $M$  antennas, respectively. The number of transmitting and receiving antennas at the  $k$ th EAP are denoted by  $N_{T,k}$  and  $N_{R,k}$ , respectively,  $\forall k \in \mathcal{K}$ , and  $N_k = N_{T,k} + N_{R,k}$ . We assume that the ST is batteryless, and thus it resorts to WEH as its only source of power for information transmission<sup>3</sup>.

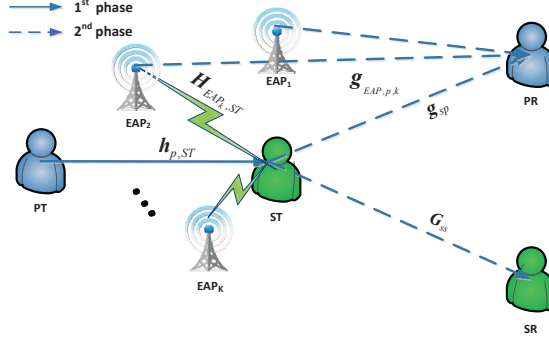


Fig. 1. System model for the wireless powered CCRN.

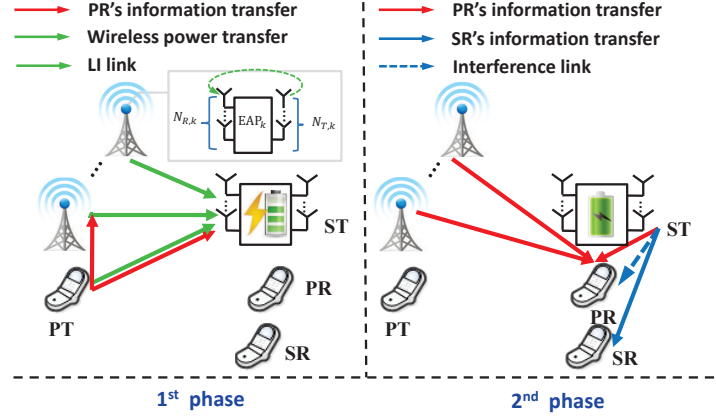


Fig. 2. Transmission protocol for the wireless powered CCRN.

As illustrated by Fig. 2, a two-slot (with equal length) transmission protocol is assumed to be adopted. In the first time slot, the PT transfers the energy-bearing primary user's signal to the ST. Concurrently, the EAPs operating in FD mode cooperate to transfer wireless power to the ST using  $N_{T,k}$ 's antennas, while jointly receiving information from the PT using  $N_{R,k}$ 's antennas. In the secondary time slot, the ST decodes and forwards PT's message and superimposes it on

<sup>3</sup>In this paper, we assume that the main energy consumption at the wireless powered ST is from its cooperative transmission, and thereby some other power deletion such as circuit operation [20], encoding/decoding and pilot transmission are ignored for simplicity of exposition. In addition, we confine our analysis to one transmission block, i.e., channel coherence time, w/o taking the initial energy storage [21, 22] into account. However, the solutions developed in the sequel are readily extended to accommodate constant circuit power consumption and/or initial power storage in more practical scenarios.

its own to broadcast to the PR and the SR. Meanwhile, the decoded PT's information is also forwarded to the PR by the EAPs that employ  $N_k$  antennas each for information transmission. Let  $s$  denote PT's transmitting signal that follows the circularly symmetric complex Gaussian (CSCG) distribution, denoted by  $s \sim \mathcal{CN}(0, 1)$ , and  $\mathbf{x} \sim \mathcal{CN}(\mathbf{0}, \mathbf{X})$ , the energy signals<sup>4</sup> coordinatedly transmitted by  $K$  EAPs, where  $\mathbf{X}$  is the covariance matrix of  $\mathbf{x}$ . On the other hand,  $\mathbf{x}$  can also be alternatively expressed by  $\mathbf{x} = [\mathbf{x}_k]_{k=1}^K$ , where  $\mathbf{x}_k \in \mathbb{C}^{N_{T,k} \times 1}$  is the energy signal transmitted by each individual EAP, and is subject to per-EAP power constraint given by  $\mathbb{E}[\|\mathbf{x}_k\|^2] \leq P_0$ ,  $\forall k \in \mathcal{K}$ .

#### A. The First Time Slot

**Received signal at the ST.** In this paper, we assume that the ST employs a dynamic power splitting (DPS) receiver [23] for EH and information decoding (ID) from the same stream of received signal, where  $\varrho$  portion of the received signal power is used to feed the energy supply while the remaining  $1 - \varrho$  for ID. As a result, the signal received by the ST is given by

$$\mathbf{y}_{ST}^{(1)} = \sqrt{1 - \varrho}(\mathbf{h}_{p,ST}\sqrt{P_p}s + \mathbf{H}_{EAP,ST}\mathbf{x} + \mathbf{n}_a) + \mathbf{n}_c, \quad (1)$$

where  $\mathbf{h}_{p,ST} \in \mathbb{C}^{N \times 1}$  denotes the complex channel from the PT to the ST;  $\mathbf{H}_{EAP,ST} = [\mathbf{H}_{EAP_1,ST}, \dots, \mathbf{H}_{EAP_K,ST}]$ ;  $\mathbf{n}_a$  denotes the additive white Gaussian noise (AWGN) at the antennas in RF-band with zero mean and variance  $\sigma_{n_a}^2$ ;  $\mathbf{n}_c$  is the RF-band to baseband signal conversion noise denoted by  $\mathbf{n}_c \sim \mathcal{CN}(\mathbf{0}, \sigma_{n_c}^2 \mathbf{I})$ . Furthermore, assuming that the linear receiving beamforming performed by the ST is  $\mathbf{u}_1^H \mathbf{y}_{ST}^{(1)}$ , where  $\mathbf{u}_1 \in \mathbb{C}^{N \times 1}$  is given by maximizing ST's signal-to-interference-plus-noise ratio (SINR) as follows.

$$\mathbf{u}_1^* = \arg \max_{\mathbf{u}_1} \frac{(1 - \varrho)P_p |\mathbf{u}_1^H \mathbf{h}_{p,ST}|^2}{\mathbf{u}_1^H ((1 - \varrho)(\mathbf{H}_{EAP,ST} \mathbf{X} \mathbf{H}_{EAP,ST}^H + \sigma_{n_a}^2 \mathbf{I}) + \sigma_{n_c}^2 \mathbf{I}) \mathbf{u}_1}, \quad (2)$$

which proves to be the eigenvector corresponding to the largest (generalized) eigenvalue of matrices  $((1 - \varrho)(\mathbf{H}_{EAP,ST} \mathbf{X} \mathbf{H}_{EAP,ST}^H + \sigma_{n_a}^2 \mathbf{I}) + \sigma_{n_c}^2 \mathbf{I}, \mathbf{h}_{p,ST} \mathbf{h}_{p,ST}^H)$ . It thus leads to the SINR at the ST in the first transmission phase given by

$$\begin{aligned} \lambda_{\max}((1 - \varrho)P_p \mathbf{A}^{-\frac{1}{2}} \mathbf{h}_{p,ST} \mathbf{h}_{p,ST}^H \mathbf{A}^{-\frac{1}{2}}) &\stackrel{(a)}{=} \lambda_{\max}((1 - \varrho)P_p \mathbf{h}_{p,ST}^H \mathbf{A}^{-1} \mathbf{h}_{p,ST}) \\ &= (1 - \varrho)P_p \mathbf{h}_{p,ST}^H \mathbf{A}^{-1} \mathbf{h}_{p,ST}, \end{aligned} \quad (3)$$

where  $\mathbf{A} = (1 - \varrho)(\mathbf{H}_{EAP,ST} \mathbf{X} \mathbf{H}_{EAP,ST}^H + \sigma_{n_a}^2 \mathbf{I}) + \sigma_{n_c}^2 \mathbf{I}$ , and (a) is due to the rank-one  $\mathbf{A}^{-\frac{1}{2}} \mathbf{h}_{p,ST} \mathbf{h}_{p,ST}^H \mathbf{A}^{-\frac{1}{2}}$ .

<sup>4</sup>Although the CSCG distributed energy signals are not optimal in term of pure WPT, we assume such distribution to exempt the dual-function EAPs from frequent switch between the CSCG and other possible signal generation and to keep its consistence with WIT.

**Received signal at the EAPs.** The received signal at the EAPs that is interfered with the energy signals transmitted by the same EAPs can be expressed in a vector form given by

$$\mathbf{y}_{EAP} = \mathbf{h}_{p,EAP}\sqrt{P_p}s + \mathbf{H}_{TR}\mathbf{x} + \mathbf{n}_{EAP}^{(1)}, \quad (4)$$

where  $\mathbf{h}_{p,EAP} = [\mathbf{h}_{p,EAP_1}^H, \dots, \mathbf{h}_{p,EAP_K}^H]^H$  with  $\mathbf{h}_{p,EAP_k} \in \mathbb{C}^{N_{R,k} \times 1}$ ,  $k \in \mathcal{K}$ , denoting the complex channel from the PT to the  $k$ th EAP;  $\mathbf{H}_{TR}$  indicates the effective loop interference (LI) channel from the transmitting to the receiving antennas of the EAPs after analogue domain SIC, in which the block matrices  $\mathbf{H}_{T_k,R_k} \in \mathbb{C}^{N_{R,k} \times N_{T,k}}$  on the diagonal of  $\mathbf{H}_{TR}$ ,  $\forall k$ , denote the intra-EAP LI channels from within the  $k$ th EAP, and the matrices  $\mathbf{H}_{T_i,R_j}$  off the diagonal,  $\forall i \neq j$ , represent the inter-EAP LI channels from the  $i$ th EAP to the  $j$ th EAP;  $\mathbf{n}_{EAP}^{(1)}$  is assumed to be the AWGN noise received at the EAPs, i.e.,  $\mathbf{n}_{EAP}^{(1)} \sim \mathcal{CN}(\mathbf{0}, \sigma_{EAP}^2 \mathbf{I})$ . Without loss of generality (w.l.o.g.),  $\mathbf{H}_{TR}$  is given by  $\mathbf{H}_{TR} = \sqrt{\varphi^2} \bar{\mathbf{H}}_{TR}$ , where each element in  $\mathbf{H}_{T_k,R_k}$ 's is a complex Gaussian RV with zero mean and variance of  $\varphi^2$ ; each element in  $\mathbf{H}_{T_i,R_j}$ 's is a complex Gaussian RV with zero mean and variance of  $\varphi^2$  multiplied by path-loss.  $\bar{\mathbf{H}}_{TR}$  denotes the normalized complex LI channel, and  $\varphi^2 \in [0, 1]$  indicates the residual LI channel gains.

It is worth noting that the analogue domain SIC is implemented though, the power level of the residual LI can still be much larger than that of the desired signal [24], i.e.,  $\varphi^2 \mathbb{E}[\|\bar{\mathbf{H}}_{TR}\mathbf{x}\|^2] \gg P_p \|\mathbf{h}_{p,EAP}\|^2$ , due to which the following concern arises. Channel estimation errors w.r.t the block diagonal matrices  $\bar{\mathbf{H}}_{T_k,R_k}$ 's cannot be neglected. Assume that the estimation of  $\bar{\mathbf{H}}_{TR}$  is given by  $\hat{\mathbf{H}}_{TR} = \bar{\mathbf{H}}_{TR} + \sqrt{\epsilon^2} \tilde{\mathbf{H}}_{TR}$  [11], where  $\hat{\mathbf{H}}_{TR}$  denotes the estimation of  $\bar{\mathbf{H}}_{TR}$ ;  $\tilde{\mathbf{H}}_{TR}$  denotes its erroneous channel, whose elements are complex Gaussian RVs with zero mean and variance of 1 in the block matrices  $\tilde{\mathbf{H}}_{T_k,R_k}$ 's, and variance of path-loss in the block matrices  $\mathbf{H}_{T_i,R_j}$ 's, respectively.  $\epsilon^2 \ll 1$  denotes the level of estimation accuracy. Hence, after analogue-to-digital conversion (ADC) [25], digital domain SIC is further applied to subtract  $\sqrt{\varphi^2} \hat{\mathbf{H}}_{TR}$  from (4). The processed signal is accordingly expressed as

$$\bar{\mathbf{y}}_{EAP} = \mathbf{h}_{p,EAP}\sqrt{P_p}s + \sqrt{\varphi^2 \epsilon^2} \tilde{\mathbf{H}}_{TR}\mathbf{x} + \mathbf{n}_{EAP}^{(1)}. \quad (5)$$

For the purpose of exposition, we denote  $\varphi\epsilon$  by  $\theta$  in the sequel.

Furthermore, since the  $K$  EAPs are coordinated, they can perform joint decoding of the PT's signal  $s$  to maximize their receiving SINR. Therefore the optimum receiving beamforming  $\mathbf{u}_2$  is designed such that

$$\text{SINR}_{EAP} = \max_{\mathbf{u}_2} \frac{P_p |\mathbf{u}_2^H \mathbf{h}_{p,EAP}|^2}{\mathbf{u}_2^H (\theta^2 \tilde{\mathbf{H}}_{TR} \mathbf{X} \tilde{\mathbf{H}}_{TR}^H + \sigma_{EAP}^2 \mathbf{I}) \mathbf{u}_2}, \quad (6)$$

which is equal to  $\lambda_{\max}(P_p \mathbf{B}^{-\frac{1}{2}} \mathbf{h}_{p,EAP} \mathbf{h}_{p,EAP}^H \mathbf{B}^{-\frac{1}{2}})$ , where  $\mathbf{B} = \theta^2 \tilde{\mathbf{H}}_{TR} \mathbf{X} \tilde{\mathbf{H}}_{TR}^H + \sigma_{EAP}^2 \mathbf{I}$ .

### B. The Second Time Slot

**Transmitted signal at the ST.** In the second time slot, the ST extracts the PR's desired message and superimposes it with its own message using dirty-paper coding (DPC) as follows [26].

$$\mathbf{x}_{ST}^{(2)} = \mathbf{w}_p s + \mathbf{q}_s, \quad (7)$$

where  $\mathbf{w}_p$  is the beamforming vector for  $s$ , while  $\mathbf{q}_s$  is the transmitted signal conveying the SR's information aimed for multiplexing MIMO transmission<sup>5</sup>, the covariance matrix of which is  $\mathbb{E}[\mathbf{q}_s \mathbf{q}_s^H] = \mathbf{Q}_s$ . As mentioned before, the transmitting power for the ST is solely supplied by its harvest power, i.e.,

$$\text{Tr}(\mathbf{Q}_s) + \|\mathbf{w}_p\|^2 \leq \eta \varrho P_{\text{EH}}(\mathbf{X}), \quad (8)$$

where  $P_{\text{EH}}(\mathbf{X}) = \text{Tr}(\mathbf{H}_{\text{EAP},ST} \mathbf{X} \mathbf{H}_{\text{EAP},ST}^H) + P_p \|\mathbf{h}_{p,ST}\|^2$  is the total wireless transferred power, and  $\eta$  denotes the EH conversion efficiency<sup>6</sup>.

**Transmitted signal at the EAPs.** In the second time slot, the EAPs cooperatively transmit the decoded PT's message to the PR using all of their  $N_k$ 's antennas via beamforming  $\mathbf{v}_p s$ , where  $\mathbf{v}_p = [\mathbf{v}_{p,1}^H, \dots, \mathbf{v}_{p,K}^H]^H$ , and  $\mathbf{v}_{p,k} \in \mathbb{C}^{N_k \times 1}$ ,  $k \in \mathcal{K}$ , represents the  $k$ th EAP's beamforming vector.

**Received signal at the PR.** In the second time slot, PR receives the forwarded PT's message from both the ST and EAPs as follows.

$$y_{PR}^{(2)} = \mathbf{g}_{sp}^H \mathbf{x}_{ST}^{(2)} + \mathbf{g}_{\text{EAP},p}^H \mathbf{v}_p s + n_{PR}^{(2)}, \quad (9)$$

where  $\mathbf{g}_{sp} \in \mathbb{C}^{N \times 1}$  is the Hermitian transpose of the complex channels from the ST to the PR,  $\mathbf{g}_{\text{EAP},p} = [\mathbf{g}_{\text{EAP},p}^H, \dots, \mathbf{g}_{\text{EAP},K,p}^H]^H$  with  $\mathbf{g}_{\text{EAP},k,p} \in \mathbb{C}^{N_k \times 1}$ ,  $k \in \mathcal{K}$ , is the Hermitian transpose of those from the EAPs to the PR, and  $n_{PR}^{(2)}$  is the AWGN at the PR denoted by  $n_{PR}^{(2)} \sim \mathcal{CN}(0, \sigma_{PR}^2)$ . Plugging (7) into (9),  $y_{PR}^{(2)}$  can be rewritten as

$$y_{PR}^{(2)} = (\mathbf{g}_{sp}^H \mathbf{w}_p + \mathbf{g}_{\text{EAP},p}^H \mathbf{v}_p) s + \mathbf{g}_{sp}^H \mathbf{q}_s + n_{PR}^{(2)}. \quad (10)$$

The receiving SINR for the PR treating the interference caused by the secondary information as noise in the second transmission slot is thus given by

$$\text{SINR}_{PR} = \frac{|\mathbf{g}_{sp}^H \mathbf{w}_p + \mathbf{g}_{\text{EAP},p}^H \mathbf{v}_p|^2}{\mathbf{g}_{sp}^H \mathbf{Q}_s \mathbf{g}_{sp} + \sigma_{PR}^2}. \quad (11)$$

<sup>5</sup>In fact,  $\mathbf{w}_p s$  and  $\mathbf{q}_s$  are transmitting signals precoded by DPC first and then multi-antenna beamforming.

<sup>6</sup>In this paper, we focus on the transceiver design of the wireless powered ST and the FD-enabled EAPs assuming a simple linear EH model. The interested reader can refer to [27, 28] for non-linear EH modelling taking the dependence of  $\eta$  on the input harvested power into account.



Accordingly, the achievable DF relaying rate for the PR, denoted by  $r_{PR}(\mathbf{X}, \varrho)$ , is given by

$$r_{PR}(\mathbf{X}, \varrho) = \min \left\{ \max \left\{ \frac{1}{2} \log_2 \left( 1 + (1 - \varrho) P_p \mathbf{h}_{p,ST}^H \mathbf{A}^{-1}(\varrho, \mathbf{X}) \mathbf{h}_{p,ST} \right), \right. \right. \\ \left. \left. \frac{1}{2} \log_2 \left( 1 + P_p \mathbf{h}_{p,EAP}^H \mathbf{B}^{-1}(\mathbf{X}) \mathbf{h}_{p,EAP} \right) \right\}, \frac{1}{2} \log_2 \left( 1 + \frac{|\mathbf{g}_{sp}^H \mathbf{w}_p + \mathbf{g}_{EAP,p}^H \mathbf{v}_p|^2}{\mathbf{g}_{sp}^H \mathbf{Q}_s \mathbf{g}_{sp} + \sigma_{PR}^2} \right) \right\}. \quad (12)$$

**Received signal at the SR.** Assuming that DPC is adopted at the ST, by which the ST encodes its own message with the interference caused by the PT's message known *a priori*, the SR is able to receive no interference as follows.

$$\mathbf{y}_{SR}^{(2)} = \mathbf{G}_{ss} \mathbf{q}_s + \mathbf{n}_{SR}^{(2)}, \quad (13)$$

where  $\mathbf{G}_{ss}$  denotes the MIMO channels between the ST and the SR and  $\mathbf{n}_{SR}^{(2)}$  is the received noise at the SR, denoted by  $\mathbf{n}_{SR}^{(2)} \sim \mathcal{CN}(0, \sigma_{SR}^2 \mathbf{I})$ . Accordingly, the achievable rate for the secondary overlay MIMO transmission, denoted by  $r_{SR}$ , is given by

$$r_{SR}(\mathbf{Q}_s) = \frac{1}{2} \log_2 \det \left( \mathbf{I} + \frac{\mathbf{G}_{ss} \mathbf{Q}_s \mathbf{G}_{ss}^H}{\sigma_{SR}^2} \right). \quad (14)$$

### III. PROBLEM FORMULATION

In this paper, we assume that the spectrum sharing CCRN of interest aims for maximizing the weighted sum-rate, i.e.,  $c_1 r_{PR}(\mathbf{X}, \varrho) + c_2 r_{SR}(\mathbf{Q}_s)$  (c.f. (12) and (14)), where  $c_1$  and  $c_2$  are weight coefficients that balance the priority of service between the primary and secondary system. Since the ST is required to assist with the primary transmission by DF relaying using its harvested power from the EAPs and the PT, we assume that the EAPs charge  $c_3 \eta \text{Tr}(\mathbf{H}_{EAP,ST} \mathbf{X} \mathbf{H}_{EAP,ST}^H)$  from the ST for its harvested power, where  $c_3$  is a cost conversion factor. Moreover, the EAPs also collaborate to help relaying PT's message thus alleviating the burden of the energy-limited ST. As a return, the ST pays the EAPs an amount of  $c_4 |\mathbf{g}_{EAP,p}^H \mathbf{v}_p|^2$  for their information transmission, where  $c_4$  represents the cost per unit of received PT's signal power (c.f. (9)). In summary, the total cost for the FD-enabled EAPs-aided CCRN is constrained by  $c_3 \eta \varrho \text{Tr}(\mathbf{H}_{EAP,ST} \mathbf{X} \mathbf{H}_{EAP,ST}^H) + c_4 |\mathbf{g}_{EAP,p}^H \mathbf{v}_p|^2 \leq C$ , where  $C$  is the total budget of the ST.

It is worth noting that this constraint will have a impact on the system only when  $C \leq C_{\max}$ , where  $C_{\max}$  denotes the maximum possible system payment given by the following problem.

$$\begin{aligned} (\text{P0}) : \max_{\mathbf{X}, \mathbf{v}_p} \quad & c_3 \eta \varrho \text{Tr}(\mathbf{H}_{EAP,ST} \mathbf{X} \mathbf{H}_{EAP,ST}^H) + c_4 |\mathbf{g}_{EAP,p}^H \mathbf{v}_p|^2 \\ \text{s.t.} \quad & \text{Tr}(\mathbf{E}_k \mathbf{X}) \leq P_0, \quad \forall k, \\ & \|\mathbf{v}_{p,k}\|^2 \leq P_0, \quad \forall k. \end{aligned}$$

Note that the addends of the objective function of Problem (P0) are independent of each other and thus can be solved separately. Specifically, the second term  $|\mathbf{g}_{EAP,p}^H \mathbf{v}_p|^2$ , which accounts for the amount of PT's signal power received by the PR, yields a closed-form solution shown below.

$$|\mathbf{g}_{EAP,p}^H \mathbf{v}_p|^2 \stackrel{(a)}{\leq} \left( \sum_{k=1}^K |\mathbf{g}_{EAP_k,p}^H \mathbf{v}_{p,k}| \right)^2 \stackrel{(b)}{\leq} \left( \sqrt{P_0} \sum_{k=1}^K \|\mathbf{g}_{EAP_k,p}\|_2 \right)^2 = P_0 \|\tilde{\mathbf{g}}_{EAP,p}\|_1^2, \quad (15)$$

where the equality in (a) holds when all  $\mathbf{g}_{EAP_k,p}^H \mathbf{v}_{p,k}$ 's are aligned in the same direction; (b) is due to Cauchy-Schwartz inequality; and  $\tilde{\mathbf{g}}_{EAP,p} = [\|\mathbf{g}_{EAP_1,p}\|_2, \dots, \|\mathbf{g}_{EAP_K,p}\|_2]^T$ . As a result, only  $\mathbf{X} \succeq \mathbf{0}$  remains to be solved by  $\max_{\text{Tr}(\mathbf{E}_k \mathbf{X}) \leq P_0, \forall k} \text{Tr}(\mathbf{H}_{EAP,ST} \mathbf{X} \mathbf{H}_{EAP,ST}^H)$ , the optimum solution of which is denoted by  $\mathbf{X}^*$ . Thus,  $C_{\max}$  turns out to be  $c_3 \eta \varrho \text{Tr}(\mathbf{H}_{EAP,ST} \mathbf{X}^* \mathbf{H}_{EAP,ST}^H) + c_4 P_0 \|\tilde{\mathbf{g}}_{EAP,p}\|_1^2$ .

Next, the weighted sum-rate maximization problem subject to the harvested power at the ST, the total payment charged by the EAPs, and the per-EAP power constraints can be formulated as follows.

$$(P1) : \max_{\mathbf{X}, \mathbf{Q}_s, \mathbf{w}_p, \mathbf{v}_p, \varrho} c_1 r_{PR}(\mathbf{X}, \varrho) + c_2 r_{SR}(\mathbf{Q}_s)$$

$$\text{s.t.} \quad \|\mathbf{v}_{p,k}\|^2 \leq P_0, \forall k, \quad (16a)$$

$$\text{Tr}(\mathbf{E}_k \mathbf{X}) \leq P_0, \forall k, \quad (16b)$$

$$\text{Tr}(\mathbf{Q}_s) + \|\mathbf{w}_p\|^2 \leq \eta \varrho P_{EH}(\mathbf{X}), \quad (16c)$$

$$c_3 \eta \varrho \text{Tr}(\mathbf{H}_{EAP,ST} \mathbf{X} \mathbf{H}_{EAP,ST}^H) + c_4 |\mathbf{g}_{EAP,p}^H \mathbf{v}_p|^2 \leq C, \quad (16d)$$

$$0 \leq \varrho \leq 1, \quad (16e)$$

$$\mathbf{X} \succeq \mathbf{0}, \mathbf{Q}_s \succeq \mathbf{0}, \quad (16f)$$

where  $\mathbf{E}_k = \text{Diag}([\mathbf{0}, \dots, \mathbf{I}_k, \dots, \mathbf{0}])$ , in which  $\text{Diag}([\cdot])$  denotes a block diagonal matrix with the block matrices on the diagonal given in  $[\cdot]$ .

In the above problem (P1), (16a) and (16b) illustrates the per-EAP power constraint for information and power transfer, respectively; (16c) indicates the transmitting power constraint of the ST subject to its harvested power from the EAPs and the PT; and (16d) constrains the cost of the CCRN system no more than a constant value  $C$ .

#### IV. JOINT OPTIMIZATION OF FD ENERGY BEAMFORMING AND DF RELAYING

In this section we investigate to solve problem (P1). First, we remove the inner  $\max(\cdot)$  in  $r_{PR}(\mathbf{X}, \varrho)$  (c.f. (12)) by recasting (P1) into two subproblems, denoting the optimum value of (P1) by  $(f^* = \max\{f_1^*, f_2^*\})$ , where  $f_1^*$  and  $f_2^*$  are the optimum value of subproblems (P1.1)

and (P1.2), respectively. They represent the cases in which the transmission rate of the first-slot DF relaying is achieved by the ST and the EAPs, respectively, depending on whether  $(1 - \varrho)\mathbf{h}_{p,ST}^H \mathbf{A}^{-1}(\varrho, \mathbf{X}) \mathbf{h}_{p,ST}$  is larger than  $\mathbf{h}_{p,EAP}^H \mathbf{B}^{-1}(\mathbf{X}) \mathbf{h}_{p,EAP}$  or not.

Problem (P1.1) based on the epigraph reformulation is given by

$$\begin{aligned} \text{(P1.1)} : \quad & \max_{\mathbf{X}, \mathbf{Q}_s, \mathbf{w}_p, \mathbf{v}_p, \varrho, t} \quad \frac{1}{2} c_1 \log_2(1+t) + c_2 r_{SR}(\mathbf{Q}_s) \\ \text{s.t.} \quad & (16a) - (16e), \end{aligned} \tag{17a}$$

$$(1 - \varrho) P_p \mathbf{h}_{p,ST}^H \mathbf{A}^{-1}(\varrho, \mathbf{X}) \mathbf{h}_{p,ST} \geq P_p \mathbf{h}_{p,EAP}^H \mathbf{B}^{-1}(\mathbf{X}) \mathbf{h}_{p,EAP}, \tag{17b}$$

$$(1 - \varrho) P_p \mathbf{h}_{p,ST}^H \mathbf{A}^{-1}(\varrho, \mathbf{X}) \mathbf{h}_{p,ST} \geq t, \tag{17c}$$

$$\frac{|\mathbf{g}_{sp}^H \mathbf{w}_p + \mathbf{g}_{EAP,p}^H \mathbf{v}_p|^2}{\mathbf{g}_{sp}^H \mathbf{Q}_s \mathbf{g}_{sp} + \sigma_{PR}^2} \geq t, \tag{17d}$$

$$\mathbf{X} \succeq \mathbf{0}, \mathbf{Q}_s \succeq \mathbf{0}, t \geq 0, \tag{17e}$$

where  $\mathbf{A}$  is related to the optimization variables  $\varrho$  and  $\mathbf{X}$ , and thus denoted by  $\mathbf{A}(\varrho, \mathbf{X})$  for the convenience of exposition, while  $\mathbf{B}$  is denoted by  $\mathbf{B}(\mathbf{X})$ .

(P1.2) is similarly given by

$$\begin{aligned} \text{(P1.2)} : \quad & \max_{\mathbf{X}, \mathbf{Q}_s, \mathbf{w}_p, \mathbf{v}_p, \varrho, t} \quad \frac{1}{2} c_1 \log_2(1+t) + c_2 r_{SR}(\mathbf{Q}_s) \\ \text{s.t.} \quad & (16a) - (16e), (17d) - (17e), \end{aligned} \tag{18a}$$

$$P_p \mathbf{h}_{p,EAP}^H \mathbf{B}^{-1}(\mathbf{X}) \mathbf{h}_{p,EAP} \geq (1 - \varrho) P_p \mathbf{h}_{p,ST}^H \mathbf{A}^{-1}(\varrho, \mathbf{X}) \mathbf{h}_{p,ST}, \tag{18b}$$

$$P_p \mathbf{h}_{p,EAP}^H \mathbf{B}^{-1}(\mathbf{X}) \mathbf{h}_{p,EAP} \geq t. \tag{18c}$$

#### A. Problem Reformulation

It is observed that  $\mathbf{X}$  and  $\varrho$  are coupled together in (17b), (17c), and (16c), which make these constraints non-convex. Hence, in this subsection, we reformulate the non-convex subproblems in a tractable way. Specifically, we propose to solve problem (P1.1) in two stages as follows. First, given  $\bar{\varrho} \in [0, 1]$ , we solve the following problem.

$$\begin{aligned} \text{(P1.1-1)} : \quad & \max_{\mathbf{X}, \mathbf{Q}_s, \mathbf{w}_p, \mathbf{v}_p, t} \quad \frac{1}{2} c_1 \log_2(1+t) + c_2 r_{SR}(\mathbf{Q}_s) \\ \text{s.t.} \quad & (16a) - (16b), (17d) - (17e), \end{aligned} \tag{19a}$$

$$(1 - \bar{\varrho}) P_p \mathbf{h}_{p,ST}^H \mathbf{A}^{-1}(\bar{\varrho}, \mathbf{X}) \mathbf{h}_{p,ST} \geq P_p \mathbf{h}_{p,EAP}^H \mathbf{B}^{-1}(\mathbf{X}) \mathbf{h}_{p,EAP}, \tag{19b}$$

$$(1 - \bar{\varrho}) P_p \mathbf{h}_{p,ST}^H \mathbf{A}^{-1}(\bar{\varrho}, \mathbf{X}) \mathbf{h}_{p,ST} \geq t, \tag{19c}$$

$$\text{Tr}(\mathbf{Q}_s) + \|\mathbf{w}_p\|^2 \leq \eta \bar{\varrho} P_{EH}(\mathbf{X}), \tag{19d}$$

$$c_3 \eta \bar{\varrho} \text{Tr}(\mathbf{H}_{EAP,ST} \mathbf{X} \mathbf{H}_{EAP,ST}^H) + c_4 |\mathbf{g}_{EAP,p}^H \mathbf{v}_p|^2 \leq C. \tag{19e}$$

Then, denoting the optimum value of problem (P1.1-1) as  $f_1(\varrho)$ , the optimum  $\varrho$  can be found by solving (P1.1-2) :  $\max_{\varrho \in [0,1]} f_1(\varrho)$  via one-dimension search over  $\varrho$ , which guarantees an  $\epsilon$ -optimum<sup>7</sup> solution. Hence, we focus on solving (P1.1-1) in the sequel.

Note that since both  $\mathbf{h}_{p,ST}^H \mathbf{A}^{-1}(\bar{\varrho}, \mathbf{X}) \mathbf{h}_{p,ST}$ , denoted by  $g_1(\mathbf{X})$ , and  $\mathbf{h}_{p,EAP}^H \mathbf{B}^{-1}(\mathbf{X}) \mathbf{h}_{p,EAP}$ , denoted by  $g_2(\mathbf{X})$ , are proved to be convex functions w.r.t  $\mathbf{X}$  (see Appendix A), the constraints given by (19b) and (19c) are in general not convex. However, (19b) is seen to admit the form of difference of convex (D.C.) functions, which falls into the category of D.C. programming [29], and thus is solvable by employing D.C. iterations [30]. Specifically, we replace the left-hand-side (LHS) of (19b) ((19c)) with its first-order Taylor expansion w.r.t.  $\bar{\mathbf{X}}$ , since it is a global lower-bound estimator of the convex function  $g_1(\mathbf{X})$  and affine. Therefore, (19b) can be transformed into the following convex constraint.

$$(1 - \bar{\varrho})P_p (g_1(\bar{\mathbf{X}}) + \Re \{ \text{Tr} (\nabla_{\mathbf{X}} g_1(\bar{\mathbf{X}})(\mathbf{X} - \bar{\mathbf{X}})) \}) \geq P_p \mathbf{h}_{p,EAP}^H \mathbf{B}^{-1}(\mathbf{X}) \mathbf{h}_{p,EAP}, \quad (20)$$

where  $\nabla_{\mathbf{X}} g_1(\mathbf{X})$ , given by

$$\nabla_{\mathbf{X}} g_1(\mathbf{X}) = -(1 - \bar{\varrho}) \mathbf{H}_{EAP,ST}^H \mathbf{A}^{-1}(\bar{\varrho}, \mathbf{X}) \mathbf{h}_{p,ST} \mathbf{h}_{p,ST}^H \mathbf{A}^{-1}(\bar{\varrho}, \mathbf{X}) \mathbf{H}_{EAP,ST}, \quad (21)$$

denotes the gradient matrix of  $g_1(\mathbf{X})$ . Accordingly, plugging the LHS of (20) into (19c), the constraint (19c) is also made convex as follows.

$$(1 - \bar{\varrho})P_p (g_1(\bar{\mathbf{X}}) + \Re \{ \text{Tr} (\nabla_{\mathbf{X}} g_1(\bar{\mathbf{X}})(\mathbf{X} - \bar{\mathbf{X}})) \}) \geq t. \quad (22)$$

It is easy to verify that satisfying constraints (20) and (22) implies feasibility of (19b) and (19c), but the converse is not necessarily true. Hence, (20) and (22) in general shrink the feasible region of (P1.1-1) unless  $\mathbf{X}^* = \bar{\mathbf{X}}$ , and only lead to its lower-bound solution, which will be discussed in detail later.

Next, we look into the constraint (17d), which is non-convex due to coupling  $\mathbf{Q}_s$  and  $t$ . To facilitate solving (P1.1-1), we decouple the numerator and the denominator of its LHS by introducing an auxiliary variable  $y > 0$  as follows.

$$|\mathbf{g}_{sp}^H \mathbf{w}_p + \mathbf{g}_{EAP,p}^H \mathbf{v}_p| \geq \sqrt{ty}, \quad (23)$$

$$\mathbf{g}_{sp}^H \mathbf{Q}_s \mathbf{g}_{sp} + \sigma_{PR}^2 \leq y, \quad (24)$$

which prove to be sufficient and necessary to replace (17d). However, as  $\sqrt{ty}$  is jointly concave w.r.t.  $t$  and  $y$  over  $t > 0$  and  $y > 0$ , (23) is still non-convex. To accommodate this constraint to the framework of convex optimization, we equivalently transform the LHS of (23) into a linear form based upon the following lemma.

<sup>7</sup> $\epsilon$ -optimum means that  $\forall \epsilon > 0$ , to achieve an objective value in the  $\epsilon$ -neighbourhood of its optimum value, there always exists a corresponding one-dimension search step length.

**Lemma 4.1:** The optimum value of (P1.1) is attained when the solution of  $\mathbf{w}_p^*$  and  $\mathbf{v}_p^*$  satisfies  $\angle(\mathbf{g}_{sp}^H \mathbf{w}_p^*) = \angle(\mathbf{g}_{EAP,p}^H \mathbf{v}_p^*)$ .

*Proof:* Please refer to Appendix B. ■

In accordance with Lemma 4.1, we have the constraint (23) equivalently expressed as

$$\Re \{ \mathbf{g}_{sp}^H \mathbf{w}_p + \mathbf{g}_{EAP,p}^H \mathbf{v}_p \} \geq \sqrt{ty}. \quad (25)$$

By rotating any solution  $\mathbf{w}_p^*$  and  $\mathbf{v}_p^*$  with a common angle of  $-\angle(\mathbf{g}_{sp}^H \mathbf{w}_p^*)$ , (23) turns out to be (25) without violating any other constraints.

To deal with the RHS of (25), i.e.,  $\sqrt{ty}$ , since it is jointly w.r.t  $t > 0$  and  $y > 0$ , its first-order Taylor expansion given by

$$\sqrt{ty} \leq \sqrt{\bar{t}\bar{y}} + \frac{1}{2}\sqrt{\frac{\bar{y}}{\bar{t}}}(t - \bar{t}) + \frac{1}{2}\sqrt{\frac{\bar{t}}{\bar{y}}}(y - \bar{y}) \quad (26)$$

serves as its upper-bound approximation, in which the equality holds if and only if  $t = \bar{t}$  and  $y = \bar{y}$ . Hence, (23) can be approximated by a convex constraint expressed as

$$\Re \{ \mathbf{g}_{sp}^H \mathbf{w}_p + \mathbf{g}_{EAP,p}^H \mathbf{v}_p \} \geq \sqrt{\bar{t}\bar{y}} + \frac{1}{2}\sqrt{\frac{\bar{y}}{\bar{t}}}(t - \bar{t}) + \frac{1}{2}\sqrt{\frac{\bar{t}}{\bar{y}}}(y - \bar{y}). \quad (27)$$

Finally, the non-convex problem (P1.1-1) is reformulated as the following convex problem.

$$\begin{aligned} \text{(P1.1-1')} : \quad & \max_{\mathbf{X}, \mathbf{Q}_s, \mathbf{w}_p, \mathbf{v}_p, t, y} \quad \frac{1}{2}c_1 \log_2(1+t) + c_2 r_{SR}(\mathbf{Q}_s) \\ \text{s.t.} \quad & (16a) - (16b), (17e), (20), (22), (24), (27), (19d) - (19e), (28a) \\ & y \geq 0. \end{aligned} \quad (28b)$$

Problem (P1.2) can also be similarly treated and transformed into a two-stage problem, for which we employ the first-order Taylor expansion of the convex function  $g_2(\mathbf{X})$  in the LHS of (18b) and (18c), respectively, to serve as their lower-bound approximation. As is done with (19b) and (19c), given any  $\varrho = \bar{\varrho}$ , (18b) and (18c) can be approximated by

$$P_p (g_2(\bar{\mathbf{X}}) + \Re \{ \text{Tr} (\nabla_{\mathbf{X}} g_2(\bar{\mathbf{X}})(\mathbf{X} - \bar{\mathbf{X}})) \}) \geq (1 - \bar{\varrho}) P_p \mathbf{h}_{p,ST}^H \mathbf{A}^{-1}(\bar{\varrho}, \mathbf{X}) \mathbf{h}_{p,ST}, \quad (29)$$

and

$$P_p (g_2(\bar{\mathbf{X}}) + \Re \{ \text{Tr} (\nabla_{\mathbf{X}} g_2(\bar{\mathbf{X}})(\mathbf{X} - \bar{\mathbf{X}})) \}) \geq t, \quad (30)$$

respectively, where  $\nabla_{\mathbf{X}} g_2(\mathbf{X})$  is given by

$$\nabla_{\mathbf{X}} g_2(\mathbf{X}) = -\theta^2 \tilde{\mathbf{H}}_{TR}^H \mathbf{B}^{-1}(\mathbf{X}) \mathbf{h}_{p,EAP} \mathbf{h}_{p,EAP}^H \mathbf{B}^{-1}(\mathbf{X}) \tilde{\mathbf{H}}_{TR}. \quad (31)$$

In addition, (P1.2) shares the same constraint (17d) with (P1.1), which can be approximated by the same constraints (24) and (27). Hence, the corresponding main stage of solving (P1.2) is given as follows.

$$\begin{aligned}
 (\text{P1.2-1}') : \quad & \max_{\mathbf{X}, \mathbf{Q}_s, \mathbf{w}_p, \mathbf{v}_p, t, y} \quad \frac{1}{2} c_1 \log_2(1+t) + c_2 r_{SR}(\mathbf{Q}_s) \\
 \text{s.t.} \quad & (16a) - (16b), (17e), (29) - (30), (24), (27), (19d) - (19e), (28b).
 \end{aligned}$$

### B. Proposed Iterative Solutions

In this subsection, we propose an iterative algorithm to solve (P1) based on investigation into the feasibility of problem (P1.1-1') and ((P1.2-1')). Due to their similar structure, we focus on studying the feasibility of (P1.1-1'), and then point out some key differences between these two problems in terms of their feasibility.

First, we solve the following feasibility problem to find a feasible  $\mathbf{X}$  to (P1.1-1').

$$\begin{aligned}
 (\text{P1.1-0}) : \quad & \text{Find a solution of } \mathbf{X} \text{ and } \mathbf{v}_p \\
 \text{s.t.} \quad & (16b), (20), (19e),
 \end{aligned} \tag{33a}$$

$$\mathbf{X} \succeq \mathbf{0}. \tag{33b}$$

Note that it is guaranteed by this step that given  $\bar{\varrho}$ , a feasible  $\mathbf{X}$  to problem (P1) exists, since for an arbitrary  $\bar{\mathbf{X}}$  satisfying (16b) and (19e), either (20) or (29) must hold. Therefore, if the  $\bar{\mathbf{X}}$  fails to make (P1.1) feasible, it must make (P1.2) feasible.

Next, applying the returned  $\mathbf{X}$  in the above problem as a new initial point of  $\bar{\mathbf{X}}$ , we aim to find feasible  $t$  and  $y$  by solving the following problem.

$$\begin{aligned}
 (\text{P1.1-0}') : \quad & \text{Find a solution of } \mathbf{X}, \mathbf{Q}_s, \mathbf{w}_p, \mathbf{v}_p, t, \text{ and } y \\
 \text{s.t.} \quad & (16a) - (16b), (17e), (20) - (22), (24), (27), (19d) - (19e), (28b).
 \end{aligned} \tag{34a}$$

It is worth noting that proper chosen of  $\bar{t}$  and  $\bar{y}$  is necessary to solve (P1.1-0'). For example, with  $\bar{\mathbf{X}}$  fixed,  $\bar{y}$  can be set as  $\sigma_{PR}^2$ , and then  $\bar{t}$  can be set as  $\max\{0, \min\{(1 - \bar{\varrho})P_p g_1(\bar{\mathbf{X}}), (\gamma^*)^2/y\}\}$ , in which  $\gamma^*$  is the optimum value of the following problem.

$$\begin{aligned}
 \max_{\mathbf{w}_p, \mathbf{v}_p} \quad & \Re \{ \mathbf{g}_{sp}^H \mathbf{w}_p + \mathbf{g}_{EAP,p}^H \mathbf{v}_p \} \\
 \text{s.t.} \quad & (16a), (19d), \\
 & \|\mathbf{w}_p\|^2 \leq \eta \bar{\varrho} P_{EH}(\mathbf{X}).
 \end{aligned}$$

Since problem (P1.1-0) and (P1.1-0') are both easily observed to be convex problems, they can be optimally solved by some optimization toolboxes such as CVX [31]. Denoting  $\mathbf{X}$ ,  $t$

and  $y$  returned by (P1.1-0') by  $\bar{\mathbf{X}}^{(0)}$ ,  $\bar{t}^{(0)}$ , and  $\bar{y}^{(0)}$ , respectively, it is easily seen that (P1.1-1') is feasible if  $\mathbf{X}$ ,  $t$ , and  $y$  take the value of  $\bar{\mathbf{X}}^{(0)}$ ,  $\bar{t}^{(0)}$ , and  $\bar{y}^{(0)}$ , respectively. Hence, it safely arrives at a feasible problem (P1.1-1') with the initial points  $\{\bar{\mathbf{X}}^{(0)}, \bar{t}^{(0)}, \bar{y}^{(0)}\}$  specified as above mentioned.

*Remark 4.1:* Although the initial points to problem (P1.2-1') can be found similarly, it is worth noting that compared with (29), (20) turns out to be more likely to be infeasible, since the LHS of (19b) is a monotonically decreasing function over  $\bar{\varrho} \in [0, 1]$ , and when  $\bar{\varrho} \rightarrow 1$ , it is hardly lower-bounded by the LHS of (20). To illustrate this, we consider the case that there is no  $\mathbf{X}$  satisfying (20) when  $\bar{\varrho} = 1$ . Hence, when infeasibility of (P1.1-0) is detected assuming that  $\varrho$  is searched in an increasing order, only (P1.2-1') needs to be solved for the rest of  $\bar{\varrho}$ .

Since (P1.1-1') and (P1.2-1') have been shown to be convex problems, and at least one of them is guaranteed to be feasible by initializing  $\{\bar{\mathbf{X}}^{(0)}, \bar{t}^{(0)}, \bar{y}^{(0)}\}$  as discussed above, an SCA-based algorithm is developed to solve (P1) as shown in Algorithm 1. The convergence behaviour of Algorithm 1 is assured by the following proposition.

*Proposition 4.1:* Monotonic convergence of solutions to problem (P1.1-1') and (P1.2-1') in Algorithm 1 is achieved, i.e.,  $1/2c_1 \log_2(1 + t^{(n)}) + c_2 r_{SR}(\mathbf{Q}_s^{(n)}) \geq 1/2c_1 \log_2(1 + t^{(n-1)}) + c_2 r_{SR}(\mathbf{Q}_s^{(n-1)})$ . Moreover, the converged solutions satisfy all the constraints as well as the Karush-Kuhn-Tucker (KKT) conditions of problem (P1.1-1) and (P1.2-1), respectively.

*Proof:* Please refer to Appendix C. ■

Next, we analyse the complexity of Algorithm 1 in terms of counting the arithmetic operations. Since most off-the-shelf convex optimization toolboxes handle the repeatedly encountered SDP using an interior-point algorithm, the worst-case complexity for solving (P1) is given by<sup>8</sup>  $\frac{1}{\beta} (L_1 \mathcal{O}(\max\{K + 4, \frac{LK}{2} + 1, N\}^4 \max\{\frac{LK}{2} + 1, N\}^{1/2}) + L_2 \mathcal{O}(\max\{K + 4, \frac{LK}{2}, N + 1\}^4 \max\{\frac{LK}{2}, N + 1\}^{1/2})) \log(1/\varepsilon)$  [32], which comprises two parts, where the former part accounts for the complexity for solving (P1.1); the latter part accounts for the complexity for solving (P1.2);  $L_1$  and  $L_2$  denote the number of iterations for the SCA in solving (P1.1-1') and (P1.2-1'), respectively;  $\beta$  controls the step length for one-dimension search over  $\rho \in [0, 1]$ ; and  $\varepsilon$  is determined by the solution accuracy.

### C. Proposed ZF-Based Solutions

In this subsection, we develop an insightful suboptimal solution that simplifies the receiving beamforming design of the full-duplex EAPs. It is seen from (6) that the incumbent design of  $\mathbf{u}_2$  depends on  $\mathbf{X}$ , which means that there will be some additional central optimization resources induced to compute  $\mathbf{u}_2$  after the problem (P1) has been solved and the optimum  $\mathbf{X}$  has been

<sup>8</sup>For the simplicity of exposition, we assume  $N_{T,1} = \dots = N_{T,K} = \frac{L}{2}$  and  $N_{R,1} = \dots = N_{R,K} = \frac{L}{2}$  in this expression.

---

**Algorithm 1** Proposed Algorithm for Solving Problem (P1)

---

**Require:**  $\bar{\varrho}$ ;  $\text{flag}_{\text{ST}} = 1$

```

1: if both (P1.1-0) and (P1.1-0') are solvable then
2:   go to 6
3: else
4:    $\text{flag}_{\text{ST}} = 0$ ;  $f_1(\bar{\varrho}) \leftarrow 0$ 
5: end if
6:  $n \leftarrow 0$ ; initialize  $\{\bar{\mathbf{X}}, \bar{t}, \bar{y}\}$  with  $\{\bar{\mathbf{X}}^{(0)}, \bar{t}^{(0)}, \bar{y}^{(0)}\}$  returned by problem (P1.1-0')
7: repeat
8:   Solve problem (P1.1-1') to obtain  $\{\mathbf{X}^{(n+1)}, t^{(n+1)}, y^{(n+1)}\}$ 
9:   Update  $\{\bar{\mathbf{X}}^{(n+1)}, \bar{t}^{(n+1)}, \bar{y}^{(n+1)}\} \leftarrow \{\mathbf{X}^{(n+1)}, t^{(n+1)}, y^{(n+1)}\}$ 
10:   $n \leftarrow n + 1$ 
11: until convergence of the objective value of (P1.1-1')
12:  $f_1(\bar{\varrho}) \leftarrow$  the optimum value of (P1.1-1')
13: Obtain  $f_1^*$  by one-dimension search over  $\varrho$ 
14: Solve problem (P1.2) using the SCA method similarly to obtain  $f_2^*$  by one-dimension search over  $\varrho$ 
Ensure:  $f^* = \max\{f_1^*, f_2^*\}$ 

```

---

returned. The broadcast of  $\mathbf{u}_2$  causes unfavourable delay particularly when  $N_{R,k}$ 's is large in practice. Hence, we design  $\mathbf{X}$  in such a way that the receiving beamforming  $\mathbf{u}_2$  can be locally decided.

To do so, let EAPs jointly decode the PT's message regardless of the residual LI. For example, an arbitrary vector align with  $\mathbf{h}_{p,EAP}$  is chosen as  $\mathbf{u}_2$ , i.e.,  $\mathbf{u}_2 = \mu \mathbf{h}_{p,EAP}$ ,  $\mu \in \mathbb{R}$ . In this way, the joint decoding can be implemented with the  $k$ th EAP having access only to its local CSI, i.e.,  $\mathbf{h}_{p,EAP_k}$ 's. Accordingly, the resulting receiving SINR at the EAPs coincides with its maximum, i.e.,  $P_p \|\mathbf{h}_{p,EAP}\|^2 / \sigma_{EAP}^2$ , if and only iff (iff)  $\mathbf{u}_2^H \tilde{\mathbf{H}}_{TR} \mathbf{X} \tilde{\mathbf{H}}_{TR}^H \mathbf{u}_2 = 0$ . Combining with  $\mathbf{u}_2 = \mu \mathbf{h}_{p,EAP}$ ,  $\mathbf{X}$  needs to be designed such that  $\mathbf{h}_{p,EAP}^H \tilde{\mathbf{H}}_{TR} \mathbf{X} \tilde{\mathbf{H}}_{TR}^H \mathbf{h}_{p,EAP} = 0$ . Defining  $\mathbf{h} = \tilde{\mathbf{H}}_{TR}^H \mathbf{h}_{p,EAP}$  with its normalized vector denoted by  $\bar{\mathbf{h}}$ , the projection matrix  $\mathbf{P} = \mathbf{I} - \bar{\mathbf{h}} \bar{\mathbf{h}}^H$  can be alternatively expressed as  $\mathbf{P} = \tilde{\mathbf{U}} \tilde{\mathbf{U}}^H$  with  $\tilde{\mathbf{U}} \in \mathbb{C}^{\sum N_{T,k} \times (\sum N_{T,k} - 1)}$  such that  $\bar{\mathbf{h}}^H \tilde{\mathbf{U}} = 0$  and  $\tilde{\mathbf{U}}^H \tilde{\mathbf{U}} = \mathbf{I}$ . The optimum structure of  $\mathbf{X}$  is then specified by the following lemma [33, Lemma 3.1].

**Lemma 4.2:** The ZF-based  $\mathbf{X}$  to (P1) is given by

$$\mathbf{X} = \tilde{\mathbf{U}} \tilde{\mathbf{X}} \tilde{\mathbf{U}}^H, \quad (35)$$

where  $\tilde{\mathbf{X}} \in \mathbb{C}^{(\sum N_{T,k} - 1) \times (\sum N_{T,k} - 1)}$  is a PSD matrix.

Applying Lemma 4.2 to Problem (P1.1), Problem (P1.1-1') can be reduced to

$$(P1.1-1'-ZF) : \max_{\tilde{\mathbf{X}}, \mathbf{Q}_s, \mathbf{w}_p, \mathbf{v}_p, t, y} \frac{1}{2} c_1 \log_2(1 + t) + c_2 r_{SR}(\mathbf{Q}_s)$$



$$\text{s.t.} \quad (16a), (24), (27), \quad (36a)$$

$$\text{Tr}(\tilde{\mathbf{U}}^H \mathbf{E}_k \tilde{\mathbf{U}} \tilde{\mathbf{X}}) \leq P_0, \quad \forall k, \quad (36b)$$

$$\begin{aligned} & (1 - \bar{\varrho})P_p \left( \tilde{g}_1(\tilde{\mathbf{X}}) + \Re \left\{ \text{Tr} \left( \nabla_{\mathbf{X}} \tilde{g}_1(\tilde{\mathbf{X}})(\tilde{\mathbf{X}} - \bar{\mathbf{X}}) \right) \right\} \right) \\ & \geq P_p \|\mathbf{h}_{p,EAP}\|^2 / \sigma_{EAP}^2, \end{aligned} \quad (36c)$$

$$(1 - \bar{\varrho})P_p \left( \tilde{g}_1(\tilde{\mathbf{X}}) + \Re \left\{ \text{Tr} \left( \nabla_{\mathbf{X}} \tilde{g}_1(\tilde{\mathbf{X}})(\tilde{\mathbf{X}} - \bar{\mathbf{X}}) \right) \right\} \right) \geq t, \quad (36d)$$

$$\text{Tr}(\mathbf{Q}_s) + \|\mathbf{w}_p\|^2 \leq \eta \bar{\varrho} P_{EH}(\tilde{\mathbf{U}} \tilde{\mathbf{X}} \tilde{\mathbf{U}}^H), \quad (36e)$$

$$c_3 \eta \bar{\varrho} \text{Tr}(\mathbf{H}_{EAP,ST} \tilde{\mathbf{U}} \tilde{\mathbf{X}} \tilde{\mathbf{U}}^H \mathbf{H}_{EAP,ST}^H) + c_4 |\mathbf{g}_{EAP,p}^H \mathbf{v}_p|^2 \leq C, \quad (36f)$$

$$\tilde{\mathbf{X}} \succeq \mathbf{0}, \mathbf{Q}_s \succeq \mathbf{0}, t \geq 0, y \geq 0, \quad (36g)$$

where  $\tilde{g}_1(\mathbf{X}) = g_1(\tilde{\mathbf{U}} \tilde{\mathbf{X}} \tilde{\mathbf{U}}^H)$ , and  $\nabla_{\mathbf{X}} \tilde{g}_1(\mathbf{X})$  denotes the gradient matrix of  $\tilde{g}_1(\mathbf{X})$  expressed as  $\nabla_{\mathbf{X}} \tilde{g}_1(\mathbf{X}) =$

$$-(1 - \bar{\varrho}) \tilde{\mathbf{U}}^H \mathbf{H}_{EAP,ST}^H \mathbf{A}^{-1}(\bar{\varrho}, \tilde{\mathbf{U}} \tilde{\mathbf{X}} \tilde{\mathbf{U}}^H) \mathbf{h}_{p,ST} \mathbf{h}_{p,ST}^H \mathbf{A}^{-1}(\bar{\varrho}, \tilde{\mathbf{U}} \tilde{\mathbf{X}} \tilde{\mathbf{U}}^H) \mathbf{H}_{EAP,ST} \tilde{\mathbf{U}}. \quad (37)$$

Similarly, Problem (P1.2-1') reduces to the following problem.

$$\begin{aligned} & \text{(P1.2-1'-ZF)} : \max_{\tilde{\mathbf{X}}, \mathbf{Q}_s, \mathbf{w}_p, \mathbf{v}_p, t, y} \frac{1}{2} c_1 \log_2(1 + t) + c_2 r_{SR}(\mathbf{Q}_s) \\ & \text{s.t.} \quad (16a), (36b), (24), (27), (36e) - (36g), \end{aligned} \quad (38a)$$

$$\frac{P_p \|\mathbf{h}_{p,EAP}\|^2}{\sigma_{EAP}^2} \geq (1 - \bar{\varrho}) P_p \mathbf{h}_{p,ST}^H \mathbf{A}^{-1}(\bar{\varrho}, \tilde{\mathbf{U}} \tilde{\mathbf{X}} \tilde{\mathbf{U}}^H) \mathbf{h}_{p,ST}, \quad (38b)$$

$$\frac{P_p \|\mathbf{h}_{p,EAP}\|^2}{\sigma_{EAP}^2} \geq t. \quad (38c)$$

Note that compared with (P1.2-1'), (P1.2-1'-ZF) admits a substantially simplified exposition because not only is there no more variable related to  $\mathbf{X}$  in the LHS of (38b) and (38c), but also they turn out to be convex. This means that there is no approximation made w.r.t  $\mathbf{X}$ , and thus (P1.2-1'-ZF) is expected to converge faster, since there are only two iterated variables remained,  $t$  and  $y$ . As the ZF-based solutions are reduced from Problem (P1), the solution and the convergence analysis are thus similar to Algorithm 1. Hence, we only present an outline of the algorithm for the proposed ZF-based solutions which is shown in Algorithm 2. The worst-case complexity using the ZF-based solutions can be analysed in analogue to that using the proposed iterative solutions, which is given by  $\frac{1}{\beta} (L'_1 \mathcal{O}(\max\{K + 5, \frac{LK}{2} - 1, N\}^4 \max\{\frac{LK}{2} - 1, N\}^{1/2}) + L'_2 \mathcal{O}(\max\{K + 3, \frac{LK}{2} - 1, N + 1\}^4 \max\{\frac{LK}{2} - 1, N + 1\}^{1/2})) \log(1/\varepsilon)$ , where  $L'_1$  and  $L'_2$  denote the number of iterations for the SCA in solving (P1.1-1'-ZF) and (P1.2-1'-ZF), respectively.

---

**Algorithm 2** Proposed ZF-Based Algorithm for Solving Problem (P1)

---

- 1: Find feasible  $\{\tilde{\mathbf{X}}, t, y\}$  to (P1.1-1'-ZF) as the initial  $\{\tilde{\mathbf{X}}^{(0)}, \bar{t}^{(0)}, \bar{y}^{(0)}\}$
- 2: Solve (P1.1-1'-ZF) using the SCA method
- 3: Solve (P1.1) to obtain  $f_1^*$  by one-dimension search over  $\varrho$
- 4: Find feasible  $\{t, y\}$  to (P1.2-1'-ZF) as the initial  $\{\bar{t}^{(0)}, \bar{y}^{(0)}\}$
- 5: Solve (P1.2-1'-ZF) using the SCA method
- 6: Solve (P1.2) to obtain  $f_2^*$  by one-dimension search over  $\varrho$

**Ensure:**  $f^* = \max\{f_1^*, f_2^*\}$

---

## V. BENCHMARK SCHEMES

In this section, two benchmark schemes are presented, where only one of the available EAPs operating in FD mode is selected to assist with the CCRN, and all the EAPs work together but operate in HD mode, respectively.

### A. Selective Non-cooperative FD Scheme

First, consider the case when only one EAP is selected in the CCRN. This is the case when joint transmission and/or detection of the WPT and WIT signals is expensive or unavailable due to extra resources (e.g., spectrum, power, centralized coordination point) or strict synchronization requirement among EAPs. The selection of the EAP is based on a simple criterion:  $\tilde{k} = \arg \max_{k \in \mathcal{K}} \|\mathbf{h}_{p,EAP_k}\|^2$ . Note that by replacing  $\mathbf{h}_{p,EAP}$  ( $\mathbf{g}_{EAP,p}$ ) with  $\mathbf{h}_{p,EAP_{\tilde{k}}}$  ( $\mathbf{g}_{EAP_{\tilde{k}},p}$ ), solving the resultant (P1) follows the same procedure as those detailed in Section IV-B, and thus is omitted here for brevity. Note that the worst-case complexity for solving (P1) based on the selective non-cooperative solutions can be attained by simply substituting  $K$  by 1 in the complexity analysis for the proposed iterative solutions.

### B. HD EB and DF Relaying

Next, consider the case when all the EAPs work under the HD mode. In this case, as DF relaying only takes place at the ST,  $r_{PR}(\mathbf{X}, \varrho)$  reduces to

$$r'_{PR}(\mathbf{X}, \varrho) = \frac{1}{2} \log_2 \left( 1 + \min \left\{ (1 - \varrho) P_p \mathbf{h}_{p,ST}^H \mathbf{A}^{-1} \mathbf{h}_{p,ST}, \frac{|\mathbf{g}_{sp}^H \mathbf{w}_p|^2}{\mathbf{g}_{sp}^H \mathbf{Q}_s \mathbf{g}_{sp} + \sigma_{PR}^2} \right\} \right). \quad (39)$$

Moreover, the total cost constraint for the HD EAPs-aided CCRN is also simplified as

$$c_3 \eta \varrho \text{Tr}(\mathbf{H}_{EAP,ST} \mathbf{X} \mathbf{H}_{EAP,ST}^H) \leq C. \quad (40)$$

Accordingly, (P1) can be equivalently recast into the following problem.

$$\begin{aligned} \text{(P1-HD)} : \quad & \max_{\mathbf{X}, \mathbf{Q}_s, \mathbf{w}_p, \varrho, t} \quad \frac{1}{2} c_1 \log_2(1+t) + c_2 r_{SR}(\mathbf{Q}_s) \\ \text{s.t.} \quad & (16b) - (16c), (17c), (16e) - (17e), (40), \end{aligned} \quad (41)$$

$$\frac{|g_{sp}^H \mathbf{w}_p|^2}{g_{sp}^H \mathbf{Q}_s g_{sp} + \sigma_{PR}^2} \geq t. \quad (42)$$

Compared with solving (P1), we use a slightly different approach to solve (P1-HD) in view of its structure. Note from (P1-HD) that as  $t$  increases, the objective value of (P1-HD) becomes larger at first. However, continuously increasing  $t$  will eventually violate (17c) and/or (42), since the LHS of both of them are easily shown to be upper-bounded. On the other hand, it is observed that a large enough  $t$  obtained by suppressing the value of  $\text{Tr}(\mathbf{Q}_s)$  may also compromise the value of  $r_{SR}(\mathbf{Q}_s)$ . Hence, it suggests that there exists a proper  $t$  that achieves the optimum value of (P1-HD). Given  $\varrho = \bar{\varrho}$  and  $t = \bar{t}$ , denote the optimum value of the following problem by  $f'_1(\bar{\varrho}, \bar{t})$ .

$$\begin{aligned} \text{(P1-HD-SDR)} : \quad & \max_{\mathbf{X}, \mathbf{Q}_s, \mathbf{W}_p} \quad \frac{1}{2} c_1 \log_2(1+\bar{t}) + c_2 r_{SR}(\mathbf{Q}_s) \\ \text{s.t.} \quad & (16b), (22), \end{aligned} \quad (43)$$

$$\text{Tr}(\mathbf{G}_{sp} \mathbf{W}_p) \geq \bar{t} (g_{sp}^H \mathbf{Q}_s g_{sp} + \sigma_{PR}^2), \quad (44)$$

$$\text{Tr}(\mathbf{Q}_s + \mathbf{W}_p) \leq \eta \bar{\varrho} P_{EH}(\mathbf{X}), \quad (45)$$

$$c_3 \eta \bar{\varrho} \text{Tr}(\mathbf{H}_{EAP,ST} \mathbf{X} \mathbf{H}_{EAP,ST}^H) \leq C, \quad (46)$$

$$\mathbf{X} \succeq \mathbf{0}, \mathbf{Q}_s \succeq \mathbf{0}, \mathbf{W}_p \succeq \mathbf{0}, \quad (47)$$

where  $\mathbf{G}_{sp} = \mathbf{g}_{sp} \mathbf{g}_{sp}^H$ , and  $\mathbf{W}_p = \mathbf{w}_p \mathbf{w}_p^H$  with its constraint  $\text{rank}(\mathbf{W}_p) = 1$  removed. Then we have the following lemma [34, Appendix A].

**Lemma 5.1:**  $f'_1(\varrho, t)$  is a concave function w.r.t  $t$ .

Note that given  $\varrho = \bar{\varrho}$  and  $t = \bar{t}$ , (22) implies (17c), and therefore leads to a lower-bound solution to (P1-HD), while imposing rank relaxation on  $\mathbf{W}_p$  in general enlarges its feasible region and thus yields an upper-bound solution to (P1-HD). The final effect of these two transformation on the objective value of problem (P1-HD) is nevertheless of no ambiguity, since the tightness of the rank relaxation in the latter holds because of the following proposition.

**Proposition 5.1:** The optimal solution to problem (P1-HD-SDR) satisfies  $\text{rank}(\mathbf{W}_p^*) = 1$  such that  $\mathbf{W}_p^* = \mathbf{w}_p^* \mathbf{w}_p^{*H}$ .

*Proof:* The proof for the rank-one property of  $\mathbf{W}^*$  is similar to [19, Appendix A], and is thus omitted here due to the length constraint of the paper. ■

As a result, we solve (P1-HD) by two-dimension search over  $\varrho$  and  $t$ , i.e.,  $f'^* = \max_{\varrho, t} f'_1(\varrho, t)$ , where  $t$  can be found by some low-complexity search such as bi-section algorithm in accordance with Lemma 5.1. Specifically, given any  $\varrho$  and  $t$ , an SDR problem shown in (P1-HD-SDR) is solved with only one SCA-approximated constraint (22). The worst-case complexity for solving (P1-HD) is accordingly given by  $\frac{L_3}{\beta} \mathcal{O}(\max\{K + 4, \frac{LK}{2}, N\}^4 \max\{\frac{LK}{2}, N\}^{1/2}) \log(t_{\max}/\beta_{\text{bi}}) \log(1/\varepsilon)$ , where  $L_3$  denotes the number of iterations for the SCA in solving (P1-HD-SDR) and  $\beta_{\text{bi}}$  represents the step length for bi-section w.r.t  $t$ .

## VI. NUMERICAL RESULTS

In this section, we evaluate the proposed joint EB and DF relaying scheme aided by multiple FD-enabled EAPs in the CCRN against the benchmark schemes. The proposed iterative solutions and the ZF-based solutions for solving (P1) in Section IV-B and Section IV-C are denoted by “FD Proposed” and “FD ZF”, respectively. For the benchmarks, the non-cooperative scheme with only one EAP associated with the ST in Section V-A is denoted by “FD Non-cooperative”, while the HD case introduced in Section V-B is denoted by “HD”.

In the following numerical examples, the parameters are set as follows unless otherwise specified. As illustrated in Fig. 2, there is one PT, one PR, each with one single antenna, and a pair of multi-antenna ST and SR equipped with  $M = 2$  and  $N = 2$  antennas, respectively. There are also  $K = 3$  EAPs each equipped with  $L = 4$  antennas, among which half of them are specified as transmitting antennas and the other half as receiving antennas, i.e.,  $N_{T,1} = N_{T,2} = N_{T,3} = 2$  and  $N_{R,1} = N_{R,2} = N_{R,3} = 2$ . The distance from the ST to the PT, PR, and SR are set as  $d_{p,ST} = 10\text{m}$ ,  $d_{sp} = 10\text{m}$  and  $d_{ss} = 10\text{m}$ . The EAPs are located within a circle centred on the ST with their radius uniformly distributed over  $[0, 10]\text{m}$ . The generated wireless channels consist of both large-scale path loss and small-scale multi-path fading. The pathloss model is given by  $A_0(d/d_0)^{-\alpha}$  with  $A_0 = -30\text{dB}$ , where  $d$  denotes the relevant distance,  $d_0 = 1\text{m}$  is a reference distance, and  $\alpha = 2.5$  is the path loss exponent factor. The small-scale fading follows *i.i.d.* Rayleigh fading with zero mean and unit variance. The effective residual LI channel gain  $\theta^2$  is set to be  $-60\text{dB}$ . The weight coefficients are assumed to be  $c_1 = c_2 = 1$ ,  $c_3 = 1$  and  $c_4 = 1$  are adopted for the cost per unit of received energy for WPT and WIT, respectively. The normalized cost, defined by  $C/C_{\max}$ , is set to be 0.1. The transmitting power is set as  $P_p = 10\text{dBm}$  and  $P_0 = 20\text{dBm}$ . The other parameters are set as follows. The RF-band AWGN noise and the RF-band to baseband conversion noise are set to be  $\sigma_{n_a}^2 = -110\text{dBm}$  and  $\sigma_{n_c}^2 = -70\text{dBm}$ , respectively;  $\sigma_{EAP}^2 = \sigma_{PR}^2 = \sigma_{SR}^2$  are all set equal to  $\sigma_{n_a}^2 + \sigma_{n_c}^2$ ; and the EH efficiency is set as  $\eta = 50\%$  [35]. The evaluation in the following examples are averaged over 300 independent channel realizations.

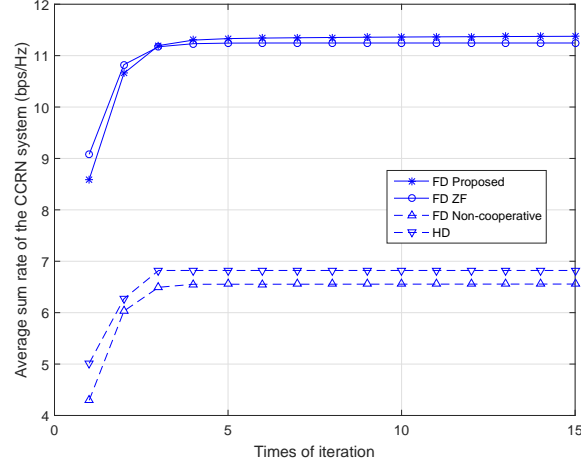


Fig. 3. The average sum-rate of the CCRN system versus the times of iteration of the SCA algorithm by the four schemes, in which  $c_1 = c_3 = c_4 = 1$  and  $c_2 = 10$ .

Fig. 3 shows the convergence behaviour of the proposed iterative algorithm, which is guaranteed by Proposition 4.1. It is also seen that the number of iterations for the proposed and the suboptimal schemes to converge is around within 10, while that for the benchmark schemes ‘FD Non-cooperative’ and ‘HD’ are less than 5. It is also observed that there is little performance gap between “FD ZF” solutions and “FD Proposed” solutions.

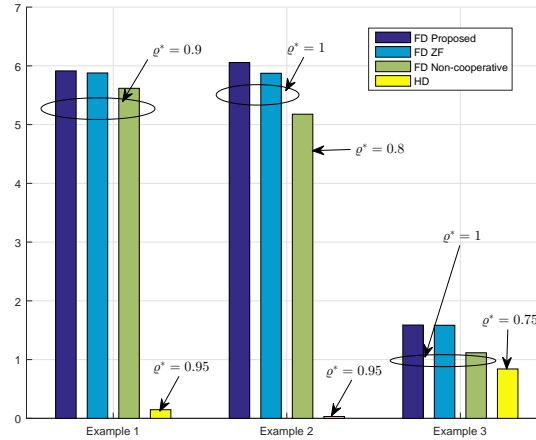


Fig. 4. The instantaneous sum-rate of the CCRN system achieved by different schemes in special scenarios, in which  $P_0 = 23\text{dBm}$  and  $P_1 = 20\text{dBm}$ .

Fig. 4 shows the instantaneous sum-rate of the system achieved by different schemes and the associated values of the PS factor  $\rho$  in some special cases. In Example 1, There are  $K = 2$  EAPs

located on the right of the ST alongside the PT-ST direction, with 10m and 20m away from the ST, respectively;  $d_{p,ST} = 5\text{m}$ ;  $N = 4$ ;  $\theta^2 = -40\text{dB}$ ;  $c_3 = 10$ ; and the normalized cost constraint is 0.01. The optimal  $\varrho$  for all the cases except the “HD” is about 0.9, which means that the ST does not exploit its full EH capability. This is mainly due to the following two reasons. On one hand, since  $\mathbf{h}_{p,ST}$  is better than  $\mathbf{h}_{p,EAP}$ , the optimum value of  $f$  is achieved by  $f_1^*$ , which means that the constraint in (17c) is active. As a result, continuing increasing  $\varrho$  will violate (17c), since it is not hard to prove that the LHS of is a monotonically decreasing function w.r.t  $\varrho \in [0, 1]$ . On the other hand, since  $c_3$  is as ten times large as  $c_4$ , which means that the unit price required by WPT is quite high, the system intuitively prefers to saving the amount of harvested power in this case. In Example 2, there are  $K = 3$  EAPs uniformly located on a circle of radius 10m centred on the ST,  $d_{p,ST} = 10\text{m}$ , and all the other settings are the same as those in Example 1. It is seen that the optimal  $\varrho$  is one in this case for both of the “FD Proposed” and “FD ZF” scheme, which is apparently due to the good channel condition of  $\mathbf{h}_{p,EAP}$ , and the enhanced  $\mathbf{H}_{EAP,ST}$ , which motivates this condition favourable to WPT.

Example 3 explores the other special case when “HD” scheme also performs reasonably well. In this case there are  $K = 5$  EAPs uniformly distributed on a circle of radius 5m centred on the ST;  $d_{ss} = 5\text{m}$ ;  $L = 2$ ,  $c_1 = 0.1$ ,  $c_2 = 1.9$ , and  $c_4 = 100$ ; and the normalized cost constraint is 0.001. Note that this case emulates the scenario when the weighted sum-rate imposes priority on the secondary system subject to a quite limited cost budget. Since the secondary system’s rate is contributed by the ST’s harvested power, the priority in favour of the ST’s transmission is achieved by splitting all its received power for EH while leaving the task of relaying the PT’s message to the EAPs.

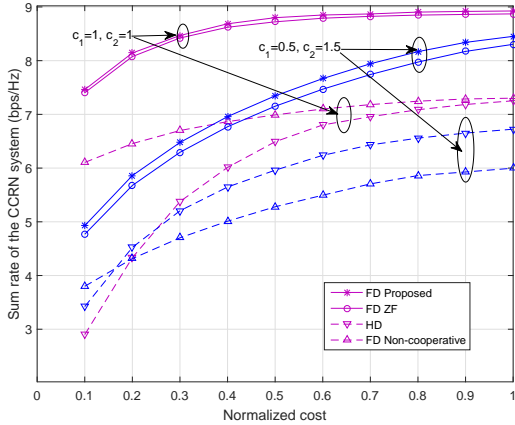
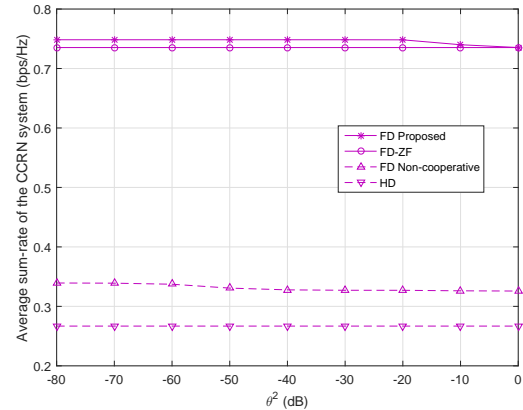
(a)  $C/C_{\max} = 0.1$ (b)  $C/C_{\max} = 0.01$ 

Fig. 5. The average sum-rate of the CCRN system versus the residue power level of the LI, in which  $d_{p,ST} = 15\text{m}$ ,  $d_{sp} = 10\text{m}$ ,  $d_{ss} = 10\text{m}$ ,  $c_1 = 0.1$ ,  $c_2 = 1.9$ ,  $c_3 = 0.1$ , and  $c_4 = 10$ ; the  $K = 3$  EAPs are located within a ST-centred circle with their radius uniformly distributed over  $[0, 5]\text{m}$ .

Fig. 5 reflects the impact of the residue power of LI on the average sum-rate of the system subject to different normalized cost constraints by different schemes. It is observed that the FD schemes are in general quite robust against the increasing power of LI. It is also seen that the suboptimal “FD ZF” approaches “FD Proposed” with negligible gap when  $\theta^2$  is larger than  $-20\text{dB}$ . This is because “FD Proposed” solutions tend to substantially suppress the LI received by the EAPs such that  $\mathbf{u}_2^{*H} \tilde{\mathbf{H}}_{TR} \mathbf{X}^* \tilde{\mathbf{H}}_{TR}^H \mathbf{u}_2^* \approx 0$  (c.f. (6)), and therefore it is overall less affected by  $\theta^2$ . In addition, “FD ZF” and “HD” schemes remain exactly the same, since their designs are irrelevant to  $\theta^2$ . Moreover, it is intriguing to see that “HD” considerably outperforms “FD Non-cooperative” in Fig. 5(a), and reversely performs in Fig. 5(b). This can be explained as follows. As a result of the transmission priority imposed on the secondary system ( $c_1 = 0.1$ ,  $c_2 = 1.9$ ), as well as the relatively cheaper per unit price for WPT ( $c_3 = 0.1$ ,  $c_4 = 10$ ), the system tends to power the ST for improving on its own transmission as much as possible. Hence, in this case, the WPT capability of “HD” is larger than that of “FD Non-cooperative”, which leads to a larger objective value that is dominated by the SR’s contribution in this case.

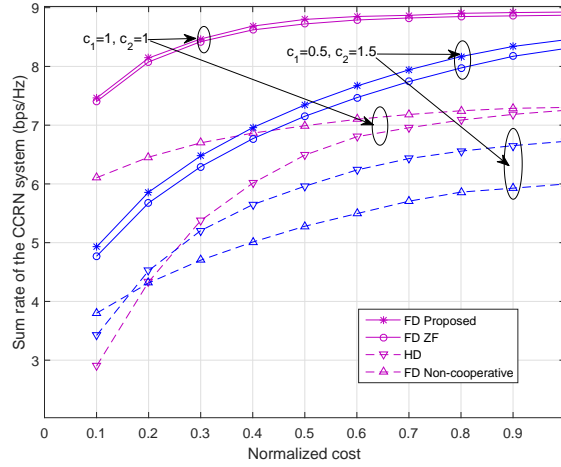


Fig. 6. The average weighted sum-rate of the CCRN system versus the normalized cost budget, in which  $K = 2$ ,  $N = 6$ ,  $c_1 = 0.5$ , and  $c_2 = 1.5$ .

Fig. 6 illustrates the average sum-rate of the system achieved by different schemes versus the normalized cost constraints with different weights of the sum-rate. It is observed that the average sum-rate of the system goes up drastically when the transmission is in favour of the ST, which is mainly caused by the imbalanced transmission efficiency between WPT and WIT. It is also observed that “FD ZF” performs nearly as well as “FD Proposed” when the primary and the secondary system share the same weights of sum-rate. This is because when  $r_{SR}(\mathbf{Q}_s)$  contributes more to the weighted sum-rate, the requirement of increasing  $\text{Tr}(\mathbf{Q}_s)$  leads to the

fact that the WPT plays a more important role in the CCRN, and therefore the suboptimal design of the WPT transmission will compromise the objective value.

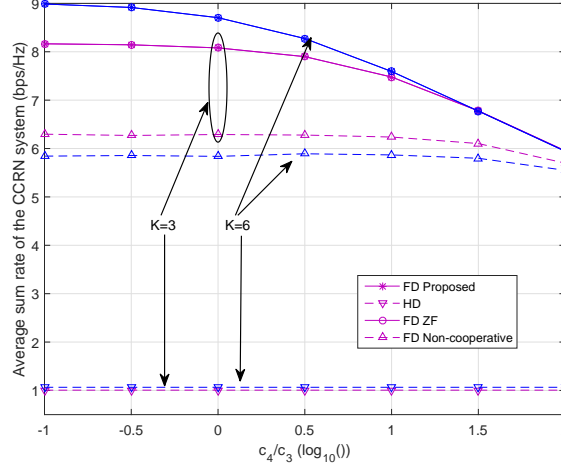


Fig. 7. The average sum-rate of the CCRN system versus the unit price of WIT normalized by that of WPT, in which  $P_p = 20\text{dBm}$  and there is a constant total cost  $C$  set to be 3.

The way that the unit price of the received energy for WIT versus WPT affects the average sum-rate of the system is shown in Fig. 7. It is seen that “FD ZF” approaches the proposed “FD Proposed” scheme with negligible gap, and both of them fall over the increasing per-unit cost for WIT, with the superior scheme of  $K = 6$  eventually decreasing to nearly the same value as that for  $K = 3$ . These observations are particularly useful when the cost for WIT is higher than that for WPT, which is usually the case in practice, since compared to coordinated WPT relying on random energy beams, it costs the EAPs more to perform WIT. In addition, “FD Non-cooperative” with  $K = 6$  EAPs is outperformed by that with  $K = 3$  EAPs, which reveals that the  $\max_{k \in \mathcal{K}} \|\mathbf{h}_{p,EAP_k}\|^2$ -based non-cooperative scheme is not an optimal strategy to fully exploit the diversity gains, since it only benefits the first hop of the DF relaying. In other words, the EAP with  $\max_{k \in \mathcal{K}} \|\mathbf{h}_{p,EAP_k}\|^2$  does not necessarily possess the maximum  $\|\mathbf{g}_{EAP_k,p}\|^2$  (c.f. (11)).

The benefit of increasing per-EAP transmission power for the average sum-rate of the system achieved by different schemes is shown in Fig. 8. It is seen that with larger number of antennas equipped at each EAP, better performance is achieved due to the increasing array gain. It is also noticed that “FD ZF” keeps up with “FD Proposed” with negligible gap until  $P_0$  increases to 20dB. Moreover, for both cases of  $L = 4$  and  $L = 6$ , it is observed that the average sum-rate achieved by all the schemes other than “FD Non-cooperative” goes up quickly as a result of the substantially enlarged feasible region (c.f. (16a)-(16b)).

Considering different sensitivities w.r.t received power for WPT and WIT, given fixed distance



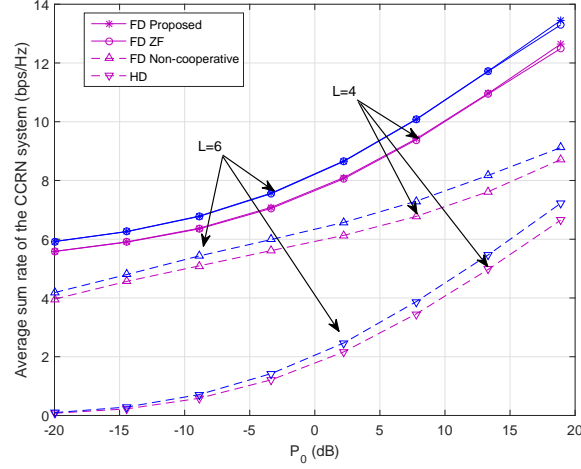


Fig. 8. The average sum-rate of the CCRN system versus the per-EAP transmit power constraint, in which  $L = 6$ .

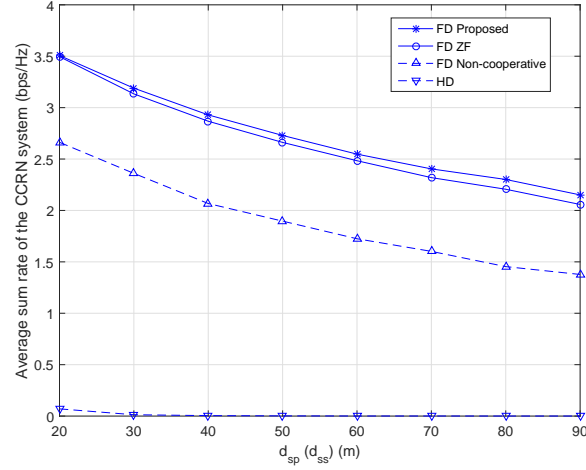


Fig. 9. The average weighted sum-rate of the CCRN system versus the WIT distance between the ST and the SR(PR), in which  $L = 6$ ,  $P_0 = 20\text{dBm}$ ,  $c_1 = 0.5$  and  $c_2 = 1.5$ .

from the PT to the ST ( $d_{p,ST} = 10\text{m}$ ), the impact of varying WIT distance (assuming  $d_{sp} = d_{ss}$ ) on the average weighted sum-rate of the CCRN system is shown in Fig. 9. It is seen that all of the schemes fall over the WIT distance, and in particular, when the Rx's are more than 30m away from the ST, "HD" cannot support effective cooperative transmission any more due to the limited harvested power at the ST.

The performance of different schemes under different number of FD-enabled EAPs is studied in Fig. 10, in which a set of EAPs with their distance to the ST drawn from uniform distribution over  $[0, 10]\text{m}$  are first deployed and then allowed to connect to the ST with an increment of one

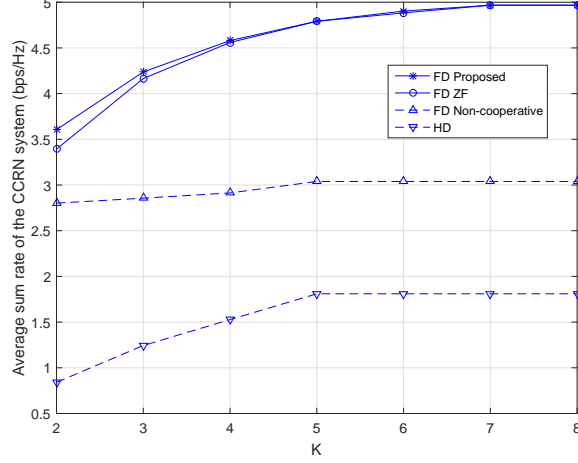


Fig. 10. The average weighted sum-rate of the CCRN system versus the number of EAPs, in which  $C = 4$ ,  $c_1 = 0.5$  and  $c_2 = 1.5$ .

EAP each time. It is observed that the advantage of cooperative gain brought by more involved EAPs is more obviously seen in the cooperative schemes than in those non-cooperative ones.

## VII. CONCLUSION

This paper investigated two techniques to fundamentally improve the spectrum efficiency of the RF EH-enabled CCRN, namely, dedicated EB and FD relaying both provided by multi-antenna EAPs. Specifically, assuming a two-equal-slot DF relaying protocol, the EAPs jointly transfer wireless power to the ST while decoding PT's message in the first transmission phase, the EAPs cooperate to forward PT's message and the ST superimposes PT's message on its own to broadcast in the second transmission phase. The EAPs' EBs as well as their receiving and transmitting beamforming for PT's message, and ST's PS ratio as well as its transmitting beamforming were jointly optimized to maximize the weighted sum-rate taking both energy and cost constraints into account. The proposed algorithms using SCA techniques were proved to converge with the KKT conditions satisfied. The EB design based on ZF was also shown to be promising. Other benchmark schemes were also provided to validate the effectiveness of the proposed ones.

## APPENDIX A CONVEXITY OF (19b)

First, the gradient of  $g_1(\mathbf{X})$  w.r.t  $\mathbf{X}$  is expressed as

$$\nabla_{\mathbf{X}} g_1(\mathbf{X}) = -(1 - \bar{\varrho}) \mathbf{H}_{EAP,ST}^H \mathbf{A}^{-1}(\bar{\varrho}, \mathbf{X}) \mathbf{h}_{p,ST} \mathbf{h}_{p,ST}^H \mathbf{A}^{-1}(\bar{\varrho}, \mathbf{X}) \mathbf{H}_{EAP,ST}. \quad (48)$$

Before obtaining the Hessian matrix of  $g_1(\mathbf{X})$  w.r.t  $\mathbf{X}$ , we derive the derivative matrix of (48) as follows.  $D(\nabla_{\mathbf{X}} g_1(\mathbf{X})) =$

$$(1 - \bar{\varrho}) \mathbf{H}_{EAP,ST}^H \mathbf{A}^{-1}(\bar{\varrho}, \mathbf{X}) D(\mathbf{A}(\bar{\varrho}, \mathbf{X})) \mathbf{A}^{-1}(\bar{\varrho}, \mathbf{X}) \mathbf{h}_{p,ST} \mathbf{h}_{p,ST}^H \mathbf{A}^{-1}(\bar{\varrho}, \mathbf{X}) \mathbf{H}_{EAP,ST} \\ + (1 - \bar{\varrho}) \mathbf{H}_{EAP,ST}^H \mathbf{A}^{-1}(\bar{\varrho}, \mathbf{X}) \mathbf{h}_{p,ST} \mathbf{h}_{p,ST}^H \mathbf{A}^{-1}(\bar{\varrho}, \mathbf{X}) D(\mathbf{A}(\bar{\varrho}, \mathbf{X})) \mathbf{A}^{-1}(\bar{\varrho}, \mathbf{X}) \mathbf{H}_{EAP,ST}. \quad (49)$$

Next, in line with the equality  $D(\mathbf{A}(\bar{\varrho}, \mathbf{X})) = (1 - \bar{\varrho}) \mathbf{H}_{EAP,ST} D\mathbf{X} \mathbf{H}_{EAP,ST}^H$ , it follows that

$$\nabla_{\mathbf{X}}^2 g_1(\mathbf{X}) = (1 - \bar{\varrho})^2 (\mathbf{A}_1^T(\bar{\varrho}, \mathbf{X}) \otimes \mathbf{A}_2(\bar{\varrho}, \mathbf{X}) + \mathbf{A}_2^T(\bar{\varrho}, \mathbf{X}) \otimes \mathbf{A}_1(\bar{\varrho}, \mathbf{X})), \quad (50)$$

where  $\mathbf{A}_1(\bar{\varrho}, \mathbf{X})$  is given by

$$\mathbf{A}_1(\bar{\varrho}, \mathbf{X}) = \mathbf{H}_{EAP,ST}^H \mathbf{A}^{-1}(\bar{\varrho}, \mathbf{X}) \mathbf{h}_{p,ST} \mathbf{h}_{p,ST}^H \mathbf{A}^{-1}(\bar{\varrho}, \mathbf{X}) \mathbf{H}_{EAP,ST}, \quad (51)$$

and  $\mathbf{A}_2 = \mathbf{H}_{EAP,ST}^H \mathbf{A}^{-1}(\bar{\varrho}, \mathbf{X}) \mathbf{H}_{EAP,ST}$ .

We can now determine the convexity of  $g_1(\mathbf{X})$  by studying the semidefiniteness of  $\nabla_{\mathbf{X}}^2 g_1(\mathbf{X})$  [36]. Take  $\mathbf{A}_1^T \otimes \mathbf{A}_2$  as an example, Since  $\lambda_l(\mathbf{A}_1^T \otimes \mathbf{A}_2) = \lambda_l(\mathbf{A}_1^T) \lambda_l(\mathbf{A}_2) \geq 0$  [37], where  $\lambda_l(\cdot)$  denotes the  $l$ th non-zero eigenvalue of the associate matrix ( $l = 1$  herein), it turns out that  $\mathbf{A}_1^T \otimes \mathbf{A}_2$  is a PSD matrix and so is  $\mathbf{A}_2^T \otimes \mathbf{A}_1$ . Hence  $\nabla_{\mathbf{X}}^2 g_1(\mathbf{X})$  is proved to be PSD and so is  $\nabla_{\mathbf{X}}^2 g_2(\mathbf{X})$ , which completes the proof.

## APPENDIX B

### PROOF OF LEMMA 4.1

This can be proved by contradiction. Assuming the optimum value of problem (P1.1) is achieved by  $\mathbf{X}^*$ ,  $\mathbf{Q}^*$ ,  $\mathbf{w}_p^*$ ,  $\mathbf{v}_p^*$ ,  $t^*$  and  $\varrho^*$  such that  $\angle(\mathbf{g}_{sp}^H \mathbf{w}_p^*) \neq \angle(\mathbf{g}_{EAP,p}^H \mathbf{v}_p^*)$ . In other words,  $\exists \mathbf{w}_p' = \mathbf{w}_p^* \exp\{j\angle\theta\}$ , where  $\theta \neq 2n\pi$ ,  $n \in \mathbb{Z}$ , such that  $\angle(\mathbf{g}_{sp}^H \mathbf{w}_p') = \angle(\mathbf{g}_{EAP,p}^H \mathbf{v}_p^*)$ . Hence, it follows that

$$|\mathbf{g}_{sp}^H \mathbf{w}_p' + \mathbf{g}_{EAP,p}^H \mathbf{v}_p^*| = (|\mathbf{g}_{sp}^H \mathbf{w}_p'| + |\mathbf{g}_{EAP,p}^H \mathbf{v}_p^*|) \exp\{j\angle(\mathbf{g}_{EAP,p}^H \mathbf{v}_p^*)\} \\ = |\mathbf{g}_{sp}^H \mathbf{w}_p^*| + |\mathbf{g}_{EAP,p}^H \mathbf{v}_p^*| \\ \stackrel{(a)}{>} |\mathbf{g}_{sp}^H \mathbf{w}_p^* + \mathbf{g}_{EAP,p}^H \mathbf{v}_p^*| \\ \geq \sqrt{t^*(\mathbf{g}_{sp}^H \mathbf{Q}_s^* \mathbf{g}_{sp} + \sigma_{PR}^2)}, \quad (52)$$

where “ $\geq$ ” in (a) holds strictly, as a result of  $\angle(\mathbf{g}_{sp}^H \mathbf{w}_p^*) \neq \angle(\mathbf{g}_{EAP,p}^H \mathbf{v}_p^*)$ . According to (52), it holds true that  $\exists \mathbf{w}_p'' = \delta \mathbf{w}_p'$ , where  $\delta \in [0, 1)$ , such that

$$|\mathbf{g}_{sp}^H \mathbf{w}_p' + \mathbf{g}_{EAP,p}^H \mathbf{v}_p^*| > |\mathbf{g}_{sp}^H \mathbf{w}_p'' + \mathbf{g}_{EAP,p}^H \mathbf{v}_p^*| = \delta |\mathbf{g}_{sp}^H \mathbf{w}_p^*| + |\mathbf{g}_{EAP,p}^H \mathbf{v}_p^*| \\ > t^*(\mathbf{g}_{sp}^H \mathbf{Q}_s^* \mathbf{g}_{sp} + \sigma_{PR}^2). \quad (53)$$

Meanwhile, we change the solution of  $\varrho^*$  to be  $\varrho'$  which is expressed as

$$\varrho' = \frac{\text{Tr}(\mathbf{Q}_s^*) + \delta^2 \|\mathbf{w}_p^*\|^2}{\text{Tr}(\mathbf{Q}_s^*) + \|\mathbf{w}_p^*\|^2} \varrho^* < \varrho^*. \quad (54)$$

So far, by changing the solution from  $\varrho^*$  to  $\varrho'$ , it is observed that the constraints (17b) and (17c) still hold, for the fact that the LHS of (17b) is a monotonically decreasing function over  $\varrho \in [0, 1]$ . Then we take the next step of changing  $t^*$  to  $t'$  as follows.

$$t' = \min \left\{ (1 - \varrho') P_p \mathbf{h}_{p,ST}^H \mathbf{A}^{-1}(\varrho', \mathbf{X}^*) \mathbf{h}_{p,ST}, \frac{|\mathbf{g}_{sp}^H \mathbf{w}_p'' + \mathbf{g}_{EAP,p}^H \mathbf{v}_p^*|^2}{\mathbf{g}_{sp}^H \mathbf{Q}_s^* \mathbf{g}_{sp} + \sigma_{PR}^2} \right\} > t^*. \quad (55)$$

Consequently, by changing the solution of  $\mathbf{w}_p^*$ ,  $\varrho^*$  and  $t^*$  to  $\mathbf{w}_p''$ ,  $\varrho'$ , and  $t'$  without changing others, we find that a larger objective value to (P1.1) is achieved without violating any other constraints, due to the increasing  $\log_2(1 + t')$ . This nevertheless contradicts to the claimed optimality achieved by  $t^*$ . Hence, the proof is complete.

## APPENDIX C

### PROOF OF PROPOSITION 4.1

Algorithm 1 will generate a sequence of feasible points  $\{\mathbf{X}^{(n)}, \mathbf{Q}_s^{(n)}, \mathbf{w}_p^{(n)}, \mathbf{v}_p^{(n)}, t^{(n)}\}$  to problem (P1.1-1), since for each iteration the feasible region to (P1.1-1') is always a subset of that to (P1.1-1). For the  $n$ th iteration,  $\{\bar{\mathbf{X}}^{(n)}, \bar{\mathbf{Q}}_s^{(n)}, \bar{\mathbf{w}}_p^{(n)}, \bar{\mathbf{v}}_p^{(n)}, \bar{t}^{(n)}\}$  is chosen as a feasible solution to (P1.1-1'), while  $\{\mathbf{X}^{(n+1)}, \mathbf{Q}_s^{(n+1)}, \mathbf{w}_p^{(n+1)}, \mathbf{v}_p^{(n+1)}, t^{(n+1)}\}$  is the returned optimal solution to (P1.1-1'). Hence, denoting the objective function of (P1.1-1') as  $h_1$  with its (implicit) dependence on the optimization variables omitted,  $h_1^{(n+1)} \geq h_1(\bar{\mathbf{X}}^{(n)}, \bar{\mathbf{Q}}_s^{(n)}, \bar{\mathbf{w}}_p^{(n)}, \bar{\mathbf{v}}_p^{(n)}, \bar{t}^{(n)}) = h_1^{(n)}$ . As a result, we arrive at a non-decreasing sequence  $\{h_1^{(n)}\}$ .

Furthermore, we show that the solutions generated by the sequence  $\{\mathbf{X}^{(n)}, \mathbf{Q}_s^{(n)}, \mathbf{w}_p^{(n)}, \mathbf{v}_p^{(n)}, t^{(n)}\}$  are bounded. In fact, the boundedness for  $\mathbf{X}^{(n)}$  and  $\mathbf{v}_p^{(n)}$  can be justified via constraints (16a) and (16b), respectively. Consequently, it holds true that the nuclear norm of  $\mathbf{Q}_s^{(n)}$  and the  $\ell^2$ -norm of  $\mathbf{w}_p^{(n)}$ , which are bounded by  $\eta \varrho P_{\text{EH}}(\mathbf{X}^{(n)})$ , is also bounded from the above. As for  $t^{(n)}$ , according to (19c), it implies that

$$\begin{aligned} t^{(n)} &\leq (1 - \bar{\varrho}) P_p \mathbf{h}_{p,ST}^H \mathbf{A}^{(n)-1} \mathbf{h}_{p,ST} \\ &\leq (1 - \bar{\varrho}) P_p \lambda_{\max}(\mathbf{A}^{(n)-1}) \|\mathbf{h}_{p,ST}\|^2 \\ &\leq (1 - \bar{\varrho}) P_p \|\mathbf{h}_{p,ST}\|^2 / (1 - \bar{\varrho}) \sigma_{na}^2 + \sigma_{nc}^2 \end{aligned} \quad (56)$$

where  $\lambda(\cdot)$  denotes the eigenvalue of the associated matrix.

Owing to the continuity of  $h_1$ , it follows that  $\{h_1^{(n)}\}$  is also bounded from the above. Hence, the non-decreasing sequence  $\{h_1^{(n)}\}$  is convergent to a real number denoted by  $h_1^*$ . Furthermore, according to Bolzano-Weierstrass theorem, the bounded sequence  $\{\mathbf{X}^{(n)}, \mathbf{Q}_s^{(n)}, \mathbf{w}_p^{(n)}, \mathbf{v}_p^{(n)}, t^{(n)}\}$  has

at least one convergent subsequence, the accumulation point of which is denoted by  $\{\mathbf{X}^*, \mathbf{Q}_s^*, \mathbf{w}_p^*, \mathbf{v}_p^*, t^*\}$ . Therefore, we automatically arrive at  $h_1(\mathbf{X}^*, \mathbf{Q}_s^*, \mathbf{w}_p^*, \mathbf{v}_p^*, t^*) = h_1^*$ . A KKT point of problem (P1.1-1), namely,  $\{\mathbf{X}^*, \mathbf{Q}_s^*, \mathbf{w}_p^*, \mathbf{v}_p^*, t^*\}$  is thus obtained [38, Theorem 1].

A similar proof can be applied to problem (P1.2-1) and is thus omitted here for brevity.

## REFERENCES

- [1] FCC, "Spectrum policy task force," Federal Communications Commission, ET Docket No. 02-135, Tech. Rep., Nov. 2002.
- [2] J. Mitola and G. Q. Maguire, "Cognitive radio: Making software radios more personal," *IEEE Pers. Commun.*, vol. 6, no. 6, pp. 13–18, Aug. 1999.
- [3] X. Kang, Y.-C. Liang, A. Nallanathan, H. K. Garg, and R. Zhang, "Optimal power allocation for fading channels in cognitive radio networks: Ergodic capacity and outage capacity," *IEEE Trans. Wireless Commun.*, vol. 8, no. 2, pp. 940–950, Feb. 2009.
- [4] J. Xu and R. Zhang, "Comp meets smart grid: A new communication and energy cooperation paradigm," *IEEE Transactions on Vehicular Technology*, vol. 64, no. 6, pp. 2476–2488, Jun. 2015.
- [5] S. Bi, Y. Zeng, and R. Zhang, "Wireless powered communication networks: an overview," *IEEE Wireless Commun.*, vol. 23, no. 2, pp. 10–18, Apr. 2016.
- [6] Wireless Power Solutions-Powercast Corp. [Online]. Available: <http://www.powercastco.com>
- [7] S. Lee, R. Zhang, and K. Huang, "Opportunistic wireless energy harvesting in cognitive radio networks," *IEEE Trans. Wireless Commun.*, vol. 12, no. 9, pp. 4788–4799, Sept. 2013.
- [8] G. Zheng, Z. Ho, E. A. Jorswieck, and B. Ottersten, "Information and energy cooperation in cognitive radio networks," *IEEE Trans. Signal Process.*, vol. 62, no. 9, pp. 2290–2303, May 2014.
- [9] S. Lee and R. Zhang, "Cognitive wireless powered network: Spectrum sharing models and throughput maximization," *IEEE Trans. Cogn. Commun. Netw.*, vol. 1, no. 3, pp. 335–346, Sept. 2015.
- [10] C. Zhai, J. Liu, and L. Zheng, "Cooperative spectrum sharing with wireless energy harvesting in cognitive radio networks," *IEEE Trans. Veh. Technol.*, vol. 65, no. 7, pp. 5303–5316, Jul. 2016.
- [11] H. Ju and R. Zhang, "Optimal resource allocation in full-duplex wireless-powered communication network," *IEEE Trans. Commun.*, vol. 62, no. 10, pp. 3528–3540, Oct. 2014.
- [12] C. Zhong, H. A. Suraweera, G. Zheng, I. Krikidis, and Z. Zhang, "Wireless information and power transfer with full duplex relaying," *IEEE Trans. Commun.*, vol. 62, no. 10, pp. 3447–3461, Oct. 2014.
- [13] Y. Zeng and R. Zhang, "Full-duplex wireless-powered relay with self-energy recycling," *IEEE Wireless Commun. Lett.*, vol. 4, no. 2, pp. 201–204, Apr. 2015.
- [14] G. Zheng, I. Krikidis, and B. Ottersten, "Full-duplex cooperative cognitive radio with transmit imperfections," *IEEE Trans. Wireless Commun.*, vol. 12, no. 5, pp. 2498–2511, May 2013.
- [15] X. Kang, C. K. Ho, and S. Sun, "Full-duplex wireless-powered communication network with energy causality," *IEEE Trans. Wireless Commun.*, vol. 14, no. 10, pp. 5539–5551, Oct. 2015.
- [16] E. Boshkovska, D. W. K. Ng, N. Zlatanov, A. Koelpin, and R. Schober, "Robust resource allocation for MIMO wireless powered communication networks based on a non-linear EH model," *to appear in IEEE Trans. Commun.*, 2017.
- [17] Y. Zeng and R. Zhang, "Optimized training design for wireless energy transfer," *IEEE Trans. Commun.*, vol. 63, no. 2, pp. 536–550, Feb. 2015.
- [18] A. Sabharwal, P. Schniter, D. Guo, D. W. Bliss, S. Rangarajan, and R. Wichman, "In-band full-duplex wireless: Challenges and opportunities," *IEEE J. Sel. Areas Commun.*, vol. 32, no. 9, pp. 1637–1652, Sept. 2014.
- [19] H. Xing, X. Kang, K.-K. Wong, and A. Nallanathan, "Optimization for DF relaying cognitive radio networks with multiple energy access points," in *Proc. IEEE Global Communications Conference (GLOBECOM)*, Wanshington, DC, USA, Dec. 2016.

- [20] D. W. K. Ng, E. S. Lo, and R. Schober, "Wireless information and power transfer: Energy efficiency optimization in OFDMA systems," *IEEE Trans. Wireless Commun.*, vol. 12, no. 12, pp. 6352–6370, Dec. 2013.
- [21] Q. Wu, M. Tao, D. W. K. Ng, W. Chen, and R. Schober, "Energy-efficient resource allocation for wireless powered communication networks," *IEEE Trans. Wireless Commun.*, vol. 15, no. 3, pp. 2312–2327, Mar. 2016.
- [22] Q. Wu, W. Chen, D. W. K. Ng, J. Li, and R. Schober, "User-centric energy efficiency maximization for wireless powered communications," *IEEE Trans. Wireless Commun.*, vol. 15, no. 10, pp. 6898–6912, Oct. 2016.
- [23] X. Zhou, R. Zhang, and C. Ho, "Wireless information and power transfer: architecture design and rate-energy tradeoff," *IEEE Trans. Commun.*, vol. 61, no. 11, pp. 4757–4767, Nov. 2013.
- [24] T. M. Kim, H. J. Yang, and A. J. Paulraj, "Distributed sum-rate optimization for full-duplex MIMO system under limited dynamic range," *IEEE Signal Process. Lett.*, vol. 20, no. 6, pp. 555–558, Jun. 2013.
- [25] B. P. Day, A. R. Margetts, D. W. Bliss, and P. Schniter, "Full-duplex bidirectional MIMO: Achievable rates under limited dynamic range," *IEEE Trans. Signal Process.*, vol. 60, no. 7, pp. 3702–3713, Jul. 2012.
- [26] G. Caire and S. Shamai, "On the achievable throughput of a multiantenna Gaussian broadcast channel," *IEEE Trans. Inf. Theory*, vol. 49, no. 7, pp. 1691–1706, Jul. 2003.
- [27] E. Boshkovska, D. W. K. Ng, N. Zlatanov, and R. Schober, "Practical non-linear energy harvesting model and resource allocation for SWIPT systems," *IEEE Commun. Lett.*, vol. 19, no. 12, pp. 2082–2085, Dec. 2015.
- [28] Y. Dong, M. J. Hossain, and J. Cheng, "Performance of wireless powered amplify and forward relaying over nakagami- $m$  fading channels with nonlinear energy harvester," *IEEE Commun. Lett.*, vol. 20, no. 4, pp. 672–675, April 2016.
- [29] A. L. Yuille and A. Rangarajan, "The concave-convex procedure," *Neural Comput.*, vol. 15, no. 4, pp. 915–936, Apr. 2003.
- [30] H. H. Kha, H. D. Tuan, and H. H. Nguyen, "Fast global optimal power allocation in wireless networks by local D.C. programming," *IEEE Trans. Wireless Commun.*, vol. 11, no. 2, pp. 510–515, Feb. 2012.
- [31] M. Grant and S. Boyd, "CVX: Matlab software for disciplined convex programming, version 2.1," <http://cvxr.com/cvx>, Jun. 2015.
- [32] Z. Luo, W. K. Ma, A. M. C. So, Y. Ye, and S. Zhang, "Semidefinite relaxation of quadratic optimization problems," *IEEE Signal Process. Mag.*, vol. 27, no. 3, pp. 20–34, May 2010.
- [33] R. Zhang, "Cooperative multi-cell block diagonalization with per-base-station power constraints," *IEEE J. Sel. Areas Commun.*, vol. 28, no. 9, pp. 1435–1445, Dec. 2010.
- [34] H. Xing, K.-K. Wong, A. Nallanathan, and R. Zhang, "Wireless powered cooperative jamming for secrecy multi-AF relaying networks," 2015, available online at arXiv:1511.03705.
- [35] A. A. Nasir, D. T. Ngo, X. Zhou, R. A. Kennedy, and S. Durrani, "Joint resource optimization for multicell networks with wireless energy harvesting relays," *IEEE Trans. Veh. Technol.*, vol. 65, no. 8, pp. 6168–6183, Aug. 2016.
- [36] S. Boyd and L. Vandenberghe, *Convex Optimization*. Cambridge Univ. Press, 2004.
- [37] R. A. Horn and C. R. Johnson, *Matrix analysis*. Cambridge uni. press, 2012.
- [38] B. R. Marks and G. P. Wright, "Technical note a general inner approximation algorithm for nonconvex mathematical programs," *Oper. Res.*, vol. 26, no. 4, pp. 681–683, 1978.